UNIVERSIDADE DE LISBOA
FACULDADE DE CIÊNCIAS
DEPARTAMENTO DE BIOLOGIA VEGETAL

Cork-associated genes in the suberization dynamics of *Arabidopsis* tissues: a contribution for their functional characterization

Ana Catarina dos Santos Vila Verde

Mestrado em Biologia Molecular e Genética

Dissertação orientada por:
Professora Doutora Célia Miguel
Professora Doutora Ana Milhinhos

2023

Acknowledgments

Em primeiro lugar, às minhas orientadoras: Professora Doutora Célia Miguel, por me receber no seu laboratório, por toda a disponibilidade para discutir o estado deste trabalho desde o início, e pela ajuda indispensável que tornou possível este trabalho; e Doutora Ana Milhinhos por ter confiado em mim para assumir este trabalho. Obrigado por todos os conselhos, sugestões, ideias, partilha do seu enorme conhecimento científico e incansável paciência ao longo de todo este trabalho, com uma enorme disponibilidade. Obrigado pela orientação que tanto me ensinou e sem a qual este trabalho não seria possível!

A todo o grupo que direta ou indiretamente contribuiu para a realização deste trabalho com os vossos conselhos e sugestões. Em especial à Raquel, que além de uma fantástica colega te tornaste numa amiga.

Aos meus Pais por serem o meu maior apoio, por todo o esforço e dedicação, ao longo de todo este trajeto.

Abstract

Cork (or phellem), from cork oak (*Quercus suber*), is produced by the secondary meristem phellogen (or cork cambium), and constitutes the external barrier that protects the tree trunk and roots. Despite its socio-economic relevance little is known about the molecular mechanisms controlling cork formation. Recently, a comparative transcriptomic study to phellogen/phellem and xylem tissues on cork oak identified a list of candidate genes involved in phellogen activity and phellem differentiation. Subsequent studies using the *Arabidopsis* root and hypocotyl models, during primary and secondary growth, identified transcription factors possibly involved in root endodermis/periderm suberization: *WOX9*/*STIP*, required for meristem growth and early development, and *ANT*, involved in floral organ development. Here we further characterize *WOX9* and *ANT* functions in *Arabidopsis* root endodermis suberization. Reverse transcription quantitative real-time-PCR analysis of root-hypocotyl tissues, targeting genes of the abscisic acid (ABA) pathway, revealed that lack of or over-expression of *WOX9* significantly affects ABA biosynthesis and signaling, suggesting *WOX9* might be a positive regulator of suberization through regulation of the ABA pathway. Additionally, we built a genetic construct expressing *QsWOX9* under CaMV35S constitutive promoter, enabling complementation experiments to study functional similarities between *Arabidopsis* and cork oak homologues. Histochemical analysis in post-embryonic ant loss-of-function roots displayed only slight reduction in suberized zones. However, through RT-qPCR targeting key genes of the suberin pathway in stem and root-hypocotyl tissues, we demonstrated that lack of *ANT* alters the expression of genes involved in biosynthesis and assembly of suberin monomers. Moreover, we showed that exogenous ABA induces suberization in ant seedlings. The expression analysis of key ABA pathway genes in *ant-9* root-hypocotyl tissues revealed the reduction of biosynthesis and downregulation of signaling, suggesting *ANT* might be a positive regulator of the ABA signaling. Overall, our results support a regulatory role for *WOX9* and *ANT* in the mechanisms underlying the suberization process.

Keywords: Periderm, endodermis, abscisic acid (ABA), suberin, transcription factor

Resumo

Os tecidos que revestem os órgãos das plantas constituem a primeira linha de defesa contra agentes bióticos e abióticos presentes no ambiente envolvente. Um dos tecidos fundamentais para essa proteção é a periderme. A periderme é formada por um conjunto de 3 tipos de tecidos: pelo felogénio, o meristema lateral que produz centripetamente a feloderme e centrifugamente o felema (ou cortiça), e surge durante o crescimento secundário das plantas. Pode revestir caules e raízes controlando as perdas de água da planta, e protegendo-a contra agentes patogénicos. A espessa camada de cortiça que se observa no sobreiro (*Quercus suber*), e que assume uma grande importância económica devido às suas várias aplicações na indústria, é consequência da capacidade do felogénio se manter ativo durante toda a longa vida da árvore. O desenvolvimento de periderme não se limita unicamente a árvores e pode também ser encontrado em espécies herbáceas como a *Arabidopsis thaliana*, planta modelo com uma crescente aplicação como ferramenta para o estudo dos mecanismos envolvidos na formação e desenvolvimento do felogénio, e no estudo da biossíntese, transporte e deposição de suberina na parede celular. A suberina é um dos principais componentes das paredes celulares das células de cortiça. É um polímero lipofílico composto por um domínio alifático e um domínio fenólico que é depositado na parede secundária, em toda a superfície da célula, contribuindo para a formação de uma barreira. A deposição de suberina não está limitada à cortiça, é também encontrada noutros tecidos que desempenham uma função protetora. Um exemplo relevante é o da suberização que ocorre nas células da endoderme da raiz, em *Arabidopsis*, onde este processo é essencial para o estabelecimento de uma barreira seletiva às trocas de água e solutos, bloqueando a difusão apoplástica. Apesar de fundamental para o sucesso da vida da planta bem como a nível socioeconómico, os mecanismos envolvidos no desenvolvimento do felogénio e diferenciação da cortiça são em grande parte ainda desconhecidos. No entanto, em 2019, um estudo de transcriptómica comparativa entre tecidos de felema/felogénio e xilema em sobreiro identificou uma lista de genes candidatos exclusivamente expressos em felema/felogénio, estando vários associados a mecanismos de suberização. A subsequente caracterização destes candidatos foi iniciada em tecidos com crescimento secundário em *Arabidopsis*, seguida do estudo do padrão de suberização das células da endoderme em plântulas com mutações nos genes candidatos identificados. Assim, foram identificados dois genes que codificam fatores de transcrição como candidatos potencialmente envolvidos no controlo da suberização da endoderme durante o desenvolvimento inicial da raiz: WUSCHEL-RELATED HOMEOBOX 9 /STIMPY (WOX9/STIP) e AINTEGUMENTA (ANT). O fator de transcrição *WOX9/STIMPY* é conhecido por promover a manutenção e crescimento dos meristemas, e os seus mutantes de perda de função (*stip-1* e *stip-2*) apresentam um atraso significativo na suberização da endoderme da raiz em plântulas enquanto que o mutante de ganho de função (*stip-D*) leva ao início precoce da suberização. Anteriormente foi demonstrado que os defeitos na suberização no mutante *stip-1* podem ser resgatados pela aplicação exógena de ácido abscísico (ABA). Para investigar se o *WOX9/STIP* estaria a interagir com a via do ABA, foi feita uma análise de expressão em tecidos de raiz e hipocótilo de mutantes de perda e ganho de função, com alvo em genes envolvidos na biossíntese (*NCED3*), sinalização (*PYR1* e *PP2CA*) e catabolismo (*CYP707A1*) do ABA, por PCR quantitativo. Os resultados revelaram uma redução de expressão de *NCED3* e *PP2CA*, enquanto que o mutante de sobrexpressão revelou uma redução de expressão do gene *PP2CA*, acompanhado por um ligeiro aumento de expressão de *PYR1* e *PP2CA*, quando comparado com o controlo do 'tipo selvagem'. Estes resultados sugerem que o *WOX9* exerce uma regulação positiva na via do ABA, direta ou indiretamente, enquanto que os resultados obtidos em *stip-D* apontam para um efeito de aumento de sinalização bem como do catabolismo do ABA. Considerando que estes genes candidatos foram inicialmente identificados em sobreiro e que a sua caracterização foi feita sobre os genes homólogos em

Arabidopsis, é necessário investigar a existência de semelhanças funcionais entre os dois homólogos. Para testar esta hipótese, o gene *WOX9/STIP* de sobreiro foi clonado sob a regulação do promotor constitutivo CaMV35S, e plantas *stip-1* e Columbia-0 foram transformadas pelo método de 'floral dipping', mediado por *Agrobacterium tumefaciens*. Estudos de caracterização do padrão de suberização nas plântulas transformadas permitirão investigar semelhanças funcionais entre as duas proteínas. O gene *ANT* codifica um fator de transcrição que está envolvido na floração controlando a proliferação celular durante o desenvolvimento floral. Análises histológicas previamente realizadas ao mutante de perda de função *ant-9* mostraram haver um atraso significativo na suberização da endoderme. Para investigar se as alterações descritas anteriormente afetam a suberização no inicio do desenvolvimento da endoderme do mutante de perda de função *ant-9*, foi feita uma análise histológica preliminar do padrão de suberização de plântulas mais jovens, adotando o método de coloração histológica por Fluorol Yellow 088 (FY), um corante fluorescente que marca especificamente a suberina, e as seedlings foram observadas através de microscopia confocal de fluorescência. A extensão da suberização da raiz em estádios de desenvolvimentos tão precoces foi determinado considerando a classificação apenas em ‘zona suberizada’ e ‘não suberizada’. A zona suberizada inclui a região de suberização "patchy" em que surgem as primeiras células suberizadas de forma aparentemente assíncrona das células adjacentes, e a zona de suberização ‘contínua’ onde todas as células que formam a endoderme estão suberizadas. Não se observaram alterações significativas nas proporções de endoderme suberizada/não-suberizada do mutante *ant-9* aos 3 dias após a germinação (DAG). Estes resultados sugerem que é possível que o ANT não atue no início da suberização da endoderme aquando da diferenciação no padrão “patchy”, mas sim regulando a entrada na sua forma contínua. Atendendo ao efeito que a falta de *ANT funcional tem* na suberização a expressão de genes da via biossintética e de deposição de suberina foi investigada, recorrendo a uma abordagem de PCR quantitativo em tempo-real em tecidos de caule e raiz-hipocótilo. Os resultados obtidos demonstram níveis de expressão muito baixos no caule, o que está de acordo com a literatura que descreve a ausência de suberização no caule de *Arabidopsis*. A expressão dos genes da via da suberina em tecidos de raiz e hipocótilo revelou que *ANT* afeta significativamente a expressão do gene *ASFT*, responsável pela ligação do ácido ferúlico aos monómeros alifáticos da via, que é reduzido significativamente relativamente ao controlo do ‘tipo selvagem’, e em *CYP86B1*, envolvido na síntese dos monómeros alifáticos, cuja expressão aumentou em relação ao controlo. O efeito observado na expressão dos genes da via da suberina sugere a regulação desta via direta ou indiretamente por *ANT*. É reconhecido que um dos mecanismos capaz de regular a suberização é através do controlo dos níveis de ABA. Para investigar se ANT regula a suberização da endoderme através da via do ABA, as plântulas de *ant-9* foram expostas durante 24h a ABA exógeno contido no meio de cultura. Ao observar as raízes e hipocótilos de *ant-9* coradas com FY ao microscópio confocal de fluorescência, verificou-se um aumento da região suberizada nas plântulas *ant-9* sujeitas a tratamento com ABA, sugerindo que o ABA reverteu o fenótipo *ant-9* e que o *ANT* pode operar a montante da via do ABA. Quando a expressão dos genes da via do ABA foi analisada por PCR quantitativo em tecidos de raiz e hipocótilo no mutante *ant-9* verificou-se uma redução de expressão do gene *NCED3* e *PP2CA* relativamente ao controlo, o que sugere uma regulação positiva destes genes pelo ANT, reduzindo a biossíntese do ABA, e curiosamente reduzindo a expressão do regulador negativo *PP2CA*, o que pode aumentar a sensibilidade ao ABA. O *ANT* é regulado pelo ABA e os resultados aqui descritos sugerem que *ANT* pode estar envolvido num loop regulatório com a via do ABA, em que *ANT* induz a expressão de alguns elementos da via. Juntamente com os resultados obtidos da análise de expressão dos genes da via da suberina, é possível que mecanismos adicionais estejam envolvidos na mesma via de regulação de *ANT*. No seu conjunto, os resultados obtidos neste trabalho constituem um progresso na compreensão da regulação da

suberização, no entanto, para definir claramente a função destes genes na suberização serão necessários estudos adicionais futuros.

Palavras-chave: Periderme, endoderme, ácido abscísico (ABA), suberina, fator de transcrição

Index

List of Figures

List of Tables

Abbreviation list

AB	Aniline Blue
ABA	Abscisic acid
ABCG	ATP-BINDING CASSETTE
ANT	AINTEGUMENTA
ASFT	Aliphatic suberin feruloyl transferase
cDNA	Complementary DNA
CDS	Coding sequence
CoA	Acyl-coenzymeA
Col-0	Columbia
CYP	Cytochrome P450
dag	Days after germination
ECR	Enoyl-CoA reductase;
EV	Extracellular vesicular-tubular structures;
EVB	Bodies containing extracellular vesicular-tubular structures
FACT	Fatty alcohol:caffeoyl-coa caffeoyl transferase
FAR	Fatty acyl-CoA reductase
FY	Fluorol Yellow 088
GELP	GDSL-type esterase/lipase proteins
GPAT	Glycerol-3-Phosphate Acyltransferase
HCD	3-hHydroxyacyl-Coa dehydratase;
KCS	β-Ketoacyl-Coa synthetase

LAC	Long-chain Acyl-Coa Synthetases
L*er*	Landsberg *erecta*
MS	Murashige and Skoog
NCED3	9-Cis epoxy carotenoid dioxygenase 3
PCR	Polymerase Chain Reaction
PP2CA	Phosphatase type 2c belonging to clade A
PPT	Phosphinotricin
PYR1	pyrabactin resistance 1
QsWOX9	*Quercus suber* WOX9 coding sequence
SPAD	Suberin poly(aliphatic) domain
SPPD	Suberin poly(phenolic) domain
WOX9	WUSCHEL-RELATED HOMEOBOX 9
WT	Wild-type

1 Introduction

1.1 Plant barrier tissues

Plants have evolved complex defense mechanisms to cope with the various biotic and abiotic challenges imposed by the environment. The first line of defense is conferred by the establishment of a robust barrier formed by the tissues covering the organs' external surface (Campilho et al., 2020; Serra et al., 2022; Serra & Geldner, 2022). The protective properties of those tissues are strongly associated with the characteristics of the cell wall's composition and structure. Lignin, cutin and suberin polymers play a relevant role in establishing and maintaining such protective barriers throughout the plant's life (Serra & Geldner, 2022). The lignin monomers are produced by the phenylpropanoid pathway, and are found in the composition of the secondary cell wall of lignified tissues, such as those of xylem tracheary elements that form wood, and provide rigidity and hydrophobic properties to the cells, while contributing to the water transport throughout the plant body (Evert et al., 2006). Cutin is a hydrophobic polyester composed mostly of long-chain hydroxy fatty acids, and, along with associated waxes, makes up most of the cuticle that covers the external surface of the epidermis of the aerial organs (Evert et al., 2006; Fich et al., 2016). Comparably, suberin is a polyester of fatty acids, differing in the presence of a polyphenolic fraction containing a significant amount of hydroxycinnamic acids (Nomberg et al., 2022; Serra & Geldner, 2022). Along with associated waxes, the suberin deposited in plant tissues contributes to the establishment of a diffusion barrier for gases, water and solutes (Andersen et al., 2015; Barberon et al., 2016; Campilho et al., 2020; Serra et al., 2022), increasing the tolerance to biotic and abiotic stresses, by limiting water loss and preventing pathogen infection (Belsson et al., 2007; Serra & Geldner, 2022).

Notably, the periderm constitutes an example of a protective tissue containing suberin, that when fully developed covers the plant organs including stems and roots. The periderm develops as part of the secondary growth processes that lead to the increase in girth of plants. This system of tissues is composed by the phellogen (or cork cambium), the circumference-like lateral meristem surrounding stems and roots that is responsible for the production of phelloderm, a parenchyma-like tissue produced centripetally, and phellem (or cork), a tissue composed of cells with highly suberized cell walls that is produced centrifugally (Evert et al., 2006). This is the outermost tissue responsible for the primary defense line when the epidermis which played that protective role during early post-embryonic development and primary growth, is damaged or broken down due to girth increase associated with the progression of the secondary growth (Evert et al., 2006; Serra et al., 2022).

1.2 The endodermis and periderm in Arabidopsis

1.2.1 The periderm development

In the past decade, *Arabidopsis thaliana* has been one of the models of choice to the study of phellem biology and the understanding of the molecular regulatory networks involved in suberin biosynthesis. In addition to the variety of molecular tools available for studies using Arabidopsis, this model plant also has secondary growth, particularly in roots and hypocotyls, showing extensive secondary xylem, secondary phloem and periderm development, that covers the roots and hypocotyls with outer layers of phellem (Figure1.1A, B) (Wunderling et al., 2018).

Periderm development in the hypocotyl is initiated with anticlinal cell divisions at the xylem pole pericycle cells and accompanied by the flattening of endodermal cells (stage 1; Figure 1.1A). This is followed by the initiation of periclinal cell divisions in the pericycle, now referred to as phellogen, and the reduction of the number of endodermal cells by programmed cell death (PCD) (stage 2). As more divisions occur, the periderm is progressively formed by the resulting multiple cell layers (at least two) while the endoderm is reduced to one or two cells (stage 3). At this stage, when no endodermal cells remain, the phellem differentiation is initiated from the phellogen (stage 4A), and the inner cortex disappears while the phellem cells increase in size (stage 4B) (Wunderling et al., 2018). As the periderm develops, the epidermis and cortex begin to break down and detach from the periderm (stage 5,), until a mature periderm is fully exposed as the outermost tissue (stage 6) (Wunderling et al., 2018). The development of the periderm in the root is similar to the process described for the hypocotyl. Initially, the pericycle cells divide anticlinally at the xylem poles (stage 1, Figure 1.1 B), and the following stages are characterized by the pericycle proliferation and reduction of the number of endodermal cells, being the former pericycle now designated as phellogen (stage 2). At this point, the epidermis and cortex break down and detach from the periderm along with the decrease of the number of endodermal cells and the formation of the first phellem cells (stages 3/4). Finally, the endodermal cells are absent and the fully differentiated periderm is the outermost protective tissue (Wunderling et al., 2018).

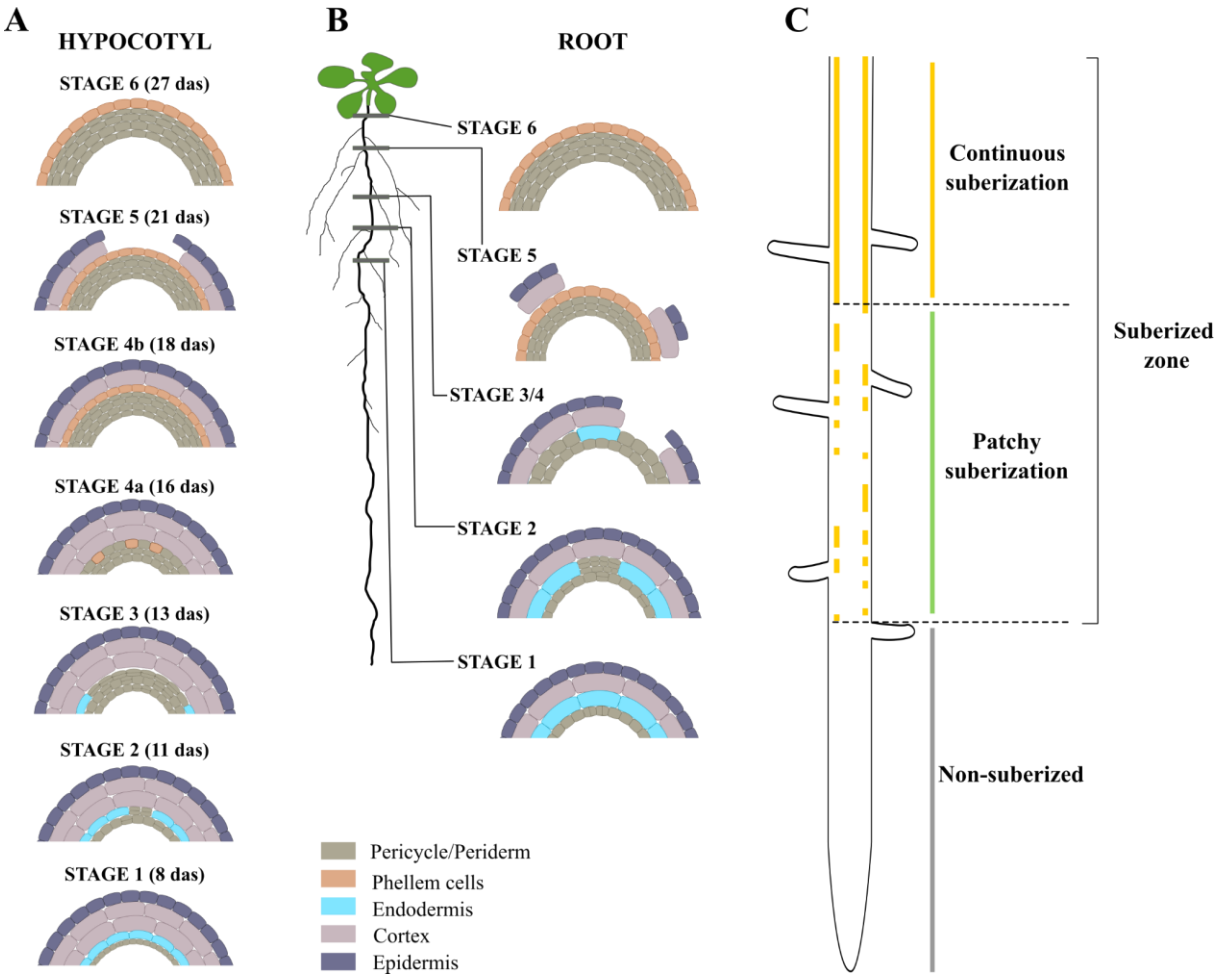

Figure 1.1 Periderm development in Arabidopsis root and hypocotyl, and endodermis differentiation. (A) Representation of the periderm development in the Arabidopsis hypocotyl: stage 1 corresponds to 8 days after sowing (das) hypocotyl, the pericycle divides anticlinal. On stage 2 (11 das) the endodermal cells begin to undergo PCD and the pericycle starts dividing

periclinally. During stage 3 (13 das) only two endodermal cells remain. Stage 4 is divided into 4a (16 das) characterized by the first identifiable phellem cells and absence of endodermal cells, and 4b (18 das) where a ring of phellem cells is formed and the inner cortex is absent. Adapted from Wunderling et al., 2018. On stage 5 (21 das) the cortex and epidermis break down and detach from the periderm. Stage 6 (27 das) shows the periderm is fully exposed as the outermost tissue. Adapted from Wunderling et al., 2018 and Campilho et al., 2020. (B) Representation of an Arabidopsis seedling. The gray bars indicate different regions corresponding to each developmental stage illustrated as root cross-sections: stage 1 is characterized by anticlinal divisions in the pericycle, in stage 2 the first periclinal divisions occur in the pericycle and endodermal cells undergo PCD, during stage 3/4 the number of endodermal cells decreases while periclinal divisions occur in the pericycle, the first phellem cells are identifiable and the epidermis and cortex begin to break exposing the periderm, on stage 5 a ring of phellem is formed and the remaining epidermis and cortex begin to detach. Stage 6 shows the periderm is fully exposed as the outermost tissue. (C) Schematic illustration of endodermis differentiation on longitudinal section of the Arabidopsis root. fluorol yellow stain (depicted in yellow) indicates endodermal cells suberization. The root endodermis suberization is divided into three identifiable zones: non-suberized zone where no FY signal is detected, patchy suberization zone in which individual cells show suberization but not the adjacent cells, continuous suberization zone where all endodermal cells show suberization. Adapted from Barberon et al., 2016.

Overall, the periderm development is similar between Arabidopsis and *Quercus suber* roots (Leal et al., 2022; Machado et al., 2013). Suberin, known for being the main component of the cell wall of *Q. suber* cork cells (Pereira, 2007), has long been identified in Arabidopsis. The genes associated with the suberin biosynthesis in Arabidopsis phellem are also found expressed in the phellem tissue of other species, such as potato (Serra, Soler, Hohn, Franke, et al., 2009; Serra, Soler, Hohn, Sauveplane, et al., 2009), cork oak (Soler et al., 2007), or *Populus* (Rains et al., 2018). This indicates that the underlying molecular mechanisms involved in the phellem development and suberization processes are possibly quite conserved among species that produce periderm. The use of such an amenable model as the Arabidopsis periderm for the study of regulatory molecular mechanisms involved in periderm development can thus be considered reliable.

1.2.2 The endodermis: differentiation in two phases

Arabidopsis roots have often been used in studies aimed to understand the molecular regulation of suberin biosynthesis, particularly during early post-embryonic development, in stages prior to the differentiation of the periderm (Barberon et al., 2016). The deposition of this polymer on the secondary cell wall of the root endodermal cells forms a diffusion barrier to water and solutes across the root tissues limited by the endodermis/pericycle (Andersen et al., 2015; Barberon et al., 2016). The differentiation of the endodermal cells is divided into two stages. The first stage (state I) is characterized by the deposition of lignin on the anticlinal primary cell walls of the endodermal cells to form the Casparian strips (Naseer et al., 2012). This structure forms a continuous ring around the cell wall joining adjacent cells and preventing apoplastic diffusion (Geldner, 2013; Naseer et al., 2012). The second stage (state II) of differentiation is identified by the deposition of suberin on the secondary cell wall of endodermal cells, differently from the Casparian strip, where suberin covers the entire inner surface of the cell wall. The suberization of the cells is a desynchronized process leading to a patch-like pattern (Figure 1.1.C; Barberon et al., 2016). Staining with the suberin lamella-specific Fluorol Yellow (FY) dye provides evidence for this pattern with identifiable regions of (i) non-suberized endodermis, on the youngest regions of the root, closer to the root apical meristem; (ii) patchy-patterned endodermis, where cells with suberized cell walls are adjacent to cells without suberization, and (iii) continuous regions, closer to the hypocotyl with continuous suberized cell walls appearance (Barberon, 2017).

1.3 The suberin biosynthesis

Suberin is a complex biopolyester consisting of an aliphatic fraction, also called the suberin poly(aliphatic) domain (SPAD), that includes long-chain fatty acids ω-hydroxyacids, dicarboxylic acids,

glycerol, and a phenolic fraction, referred to as the suberin poly(phenolic) domain (SPPD), characterized by high levels of hydroxycinnamic acids (mostly ferulic acid), that are deposited in the secondary cell wall forming a lamellar structure that can be detected through transmission electron microscopy showing a lamellae of electron opaque (dark) and electron translucent (light) layers (Graça, 2015; Holloway, 1983; Kolattukudy et al., 1975; Moire et al., 1983; Schmidt & Schönherr, 1982).

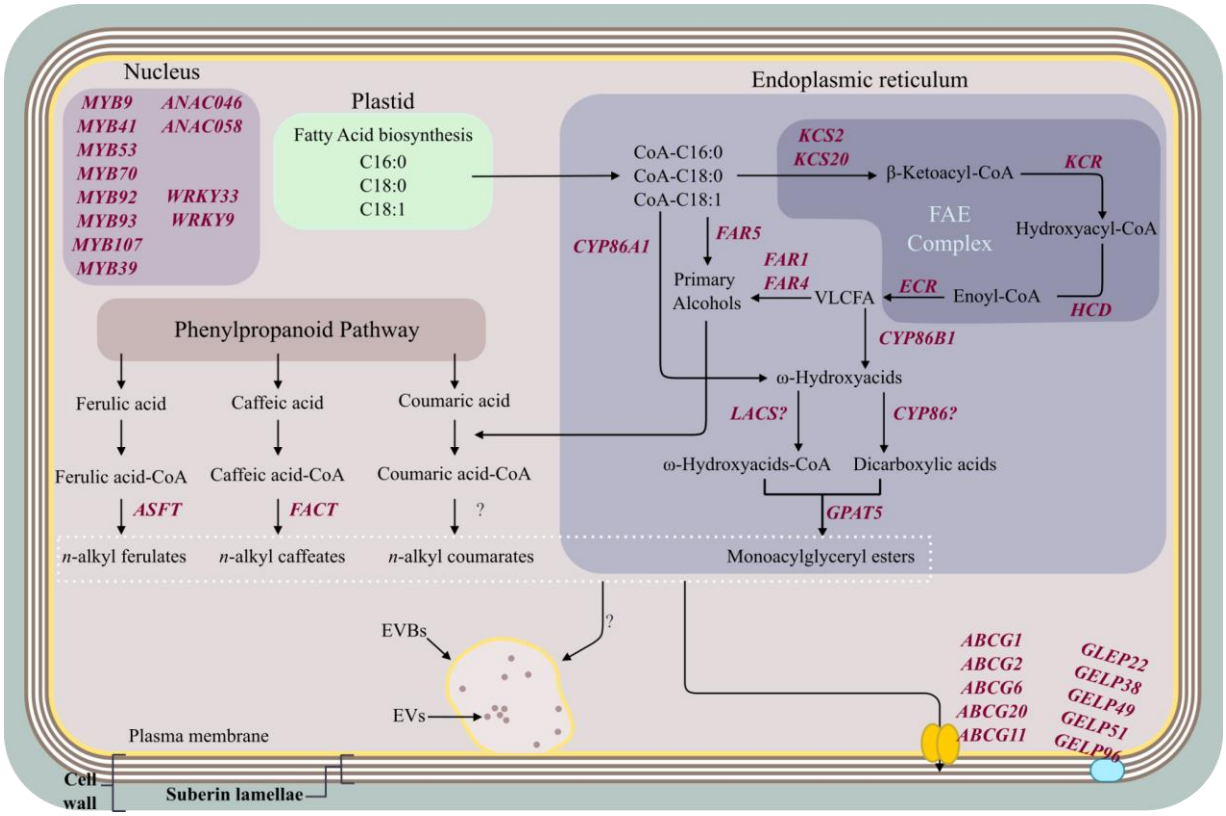

Figure 1.2 Simplified schematic illustration of the suberin pathway in Arabidopsis. The synthesis of the aliphatic suberin monomers is initiated with the synthesis of fatty acids in the plastid which are transported to the endoplasmic reticulum where the fatty acid elongation is catalyzed by the four enzymes of the Fatty acid elongation (FAE) complex, producing very long chain fatty acids, which can then lead to the production of primary alcohols by FAR enzymes, or CYPs enzymes can catalyze the producing ω-hydroxyacids and dicarboxylic acids. ω -hydroxyacids can undergo esterification with glycerol catalyzed by GPAT enzymes. The phenolic components of suberin derive from the phenylpropanoid pathway, ASFT and FACT are transferases that link the ferulic acid and caffeic acid to fatty alcohols. The transport of suberin monomers to the apoplast, to be incorporated in the cell wall is promoted by ABCG transporters. Extracellular vesicular-tubular structures have also been associated with suberin deposition. On the cell wall GELPs mediate the suberin polymerization. The white stripes on the suberin lamellae represent the light lamellae formed by the aliphatic portion of suberin, the brown stripes represent the dark lamellae formed by polyaromatics. Genes encoding enzymes involved in each step are: ASFT, ALIPHATIC SUBERIN FERULOYL TRANSFERASE; CYP, CYTOCHROME P450 (FATTY ACYL ω-HYDROXYLASE); ECR, ENOYL-CoA REDUCTASE; EV, extracellular vesicular-tubular structures; EVB, Bodies containing extracellular vesicular-tubular structures; FACT, FATTY ALCOHOL:CAFFEOYL-CoA CAFFEOYL TRANSFERASE; FAR, FATTY ACYL-CoA REDUCTASE; GELP, GDSL-type ESTERASE/LIPASE PROTEINS; GPAT, GLYCEROL-3-PHOSPHATE ACYLTRANSFERASE; HCD, 3-HYDROXYACYL-CoA DEHYDRATASE; KCR, β-KETOACYL REDUCTASE; KCS, β-KETOACYL-CoA SYNTHETASE; LAC, LONG-CHAIN ACYL-CoA SYNTHETASES. This illustration is based on previous literature. Adapted from De Bellis et al., 2022, Nomberg et al., 2022, Vishwanath et al., 2015.

The next step is oxidation, catalyzed by enzymes of the cytochrome P450 oxidase family, leading to the production of ω-hydroxyacids and α,ω-dicarboxylic acids. In Arabidopsis roots, CYP86A1 is responsible for the formation of shorter-chain ω-hydroxyacids (shorter than C20) while CYP86B1 catalyzes the formation of very long-chain ω-hydroxyacids (C22 and C24) (Compagnon et al., 2009; Kushiro et al., 2004). The primary alcohols found in the SPAD result from the reduction of fatty acids

mediated by FATTY ACYL-COA REDUCTASES (FAR). In Arabidopsis, FAR1 enzyme is involved in generating C22:0 primary alcohol, FAR4 generates C20:0 primary alcohols and FAR5 is relevant for the formation of C18:0 primary alcohols (Domergue et al., 2010). Esterification with glycerol allows the assembly of suberin molecules by linking together aliphatic monomers (Moire et al., 1983). The GLYCEROL 3-PHOSPHATE ACYLTRANSFERASES (GPATs) catalyze the last step of suberin biosynthesis, producing the monoacylglycerols which are found in suberin. In roots and seeds of Arabidopsis, GPAT5 is involved in the suberin pathway (Belsson et al., 2007). Similarly, the main phenolic monomers are also linked to the aliphatic monomers. The ALIPHATIC SUBERIN FERULOYL TRANSFERASE (ASFT) mediates the transference of feruloyl to the aliphatic monomers in Arabidopsis (Molina et al., 2009), while the FATTY ALCOHOL:CAFFEOYL-CoA CAFFEOYL TRANSFERASE (FACT) is responsible for the synthesis of alkyl hydroxycinnamate ester waxes (Figure 1.2 (Kosma et al., 2012). The polyphenolic monomers of the SPPD are mostly hydroxycinnamic acids that are produced in the phenylpropanoid pathway that is shared with the lignin biosynthesis, and include ferulic acid, caffeic acid and p-coumaric acid (Nomberg et al., 2022).

To enable suberin polymerization, the different suberin monomers must be transported into the apoplast. The half-size ATP-BINDING CASSETTE (ABCG) transporters have been implicated in the transport of suberin aliphatic monomers. In Arabidopsis the transporters ABCG1/2/6/20 and ABCG11 were shown to be involved to some extent in the suberin monomer transport (Figure 1.2) (Shanmugarajah et al., 2019; Yadav et al., 2014). However, the triple mutant *abcg2 abcg6 abcg20* was capable of suberin deposition, although with altered structure, which suggests the involvement of other transporters (Yadav et al., 2014). Another mechanism proposed to be involved in transporting the suberin monomers to the apoplastic space is a secretory pathway mediated by extracellular vesicular-tubular structures. These are membrane encapsulated structures that contain the suberin monomers, transporting them to the plasma membrane where the monomers are released to the apoplastic space (De Bellis et al., 2022).

Once the monomers reach the apoplast, the suberin polymerization takes place. The assembly of the monomers is mediated by GDSL-type esterase/lipase proteins (GELPs), GELP22, GELP38, GELP49, GELP51 and GELP96, which were demonstrated to impact suberin deposition in Arabidopsis, with GELP38, GELP49, GELP96 as endodermis-specific (Ursache et al., 2021).

1.4 Suberin regulation

1.4.1 Transcription factors

The biosynthesis of both aliphatic and phenolic compounds, its transport and polymerization require a complex regulation of the enzymes involved in the pathway. Despite the progress made in the past decade to identify regulators of the suberization process in different species, many details of these regulatory networks remain unknown (Vishwanath et al., 2015). The myeloblastosis-related (MYB), NAC domain and WRKY families of transcription factors are involved in the regulation of the suberin biosynthesis in Arabidopsis. Several members of the MYB family have been shown to be involved in the suberization process, with MYB41 inducing the synthesis and deposition of suberin aliphatic components, promoting the suberization of the root endodermis in association with MYB53, MYB92 and MYB93 (Kosma et al., 2014; Shukla et al., 2021). MYB9 and MYB107 regulate the synthesis, transport and polymerization of aliphatic and phenolic compounds on the seed coat cells (Lashbrooke et al., 2016). The regulation of suberin deposition by MYB107 and SUBERMAN/MYB39 in roots

occurs by direct binding to the promoters of suberin biosynthetic genes (Cohen et al., 2020; Gou et al., 2017). In contrast with other transcription factors, in Arabidopsis roots, MYB70 is a negative regulator of the suberin-related genes (Wan et al., 2021). The ANAC046 promoter from the NAC family is expressed in the root endodermis and promotes the suberin biosynthesis and deposition suggesting it might be acting as a transcriptional activator (Mahmood et al., 2019). Two transcription factors from the WRKY family are involved in regulating the suberin deposition in Arabidopsis roots. While WRKY33 regulates the suberin deposition through the control of CYP94B1 oxidase which is involved in suberin biosynthesis, WRKY9 regulates CYP94B3 and CYP86B1 suggesting WRKY9 controls suberization upstream (Krishnamurthy et al., 2020, 2021).

1.4.2 Phytohormones

Phytohormones are involved in the regulation of many developmental and physiological processes, including the modulation of suberin biosynthesis and deposition. The abscisic acid (ABA) is involved in the suberization process, often associated to a stress response. ABA is implicated in the suberization of the outer cells of the *Agrobacterium tumefaciens*-induced tumor in Arabidopsis, by up-regulating genes associated with the suberin biosynthesis, as a response to drought stress in this structure (Efetova et al., 2007). Upon nutrient stresses, ABA induces suberization of developing root endodermal cells in Arabidopsis (Barberon et al., 2016). Conversely, ethylene is associated with a decrease of suberization in the endodermis of developing roots, through a decrease in the suberin biosynthesis and induction of suberin lamellae degradation (Barberon et al., 2016). This regulation exerted by the phytohormones, particularly by the ABA, is closely associated with the activity of other regulatory elements. That is the case of MYB41 whose endodermal expression is triggered by ABA (Kosma et al., 2014), and MYB39, which is implicated in the endodermis suberization, in addition to its interaction with upstream factors also being induced by ABA (Wang et al., 2020).

1.4.3 Detailing the suberin regulatory network

The first periderm in most woody plants serves its purpose for a limited, species-dependent period, after which it ceases to function and is progressively replaced by new periderms. Over time, these successive periderms accumulate to form the rhytidome, which comprises multiple layers of non-functional periderms (Evert et al., 2006; Pereira, 2007). Interestingly, some plants develop a first periderm that is capable of remaining functional throughout the plant's life, continuously adding new cells to the phellem over time (Evert et al., 2006). This continuous growth over the years forms a thick layer of phellem protecting the outer surface of the stems and roots. A notorious example of a persistent periderm can be observed in the *Quercus suber* (cork oak), found in the Western Mediterranean region, Portugal, Spain, certain regions of France and Italy and North Africa (Pereira, 2007). The cork is harvested periodically, and the first cork removed, known as "virgin" cork, is of lower quality. Subsequently, the exposed phellogen dies and a new traumatic phellogen is formed in response to the trauma, resulting in higher quality "amadia" cork (Pereira, 2007). The commercial value of cork is associated with its high impermeability to gases and water and its mechanical properties, supplying many industrial sectors including construction materials, cork stoppers for the wine industry (Silva et al., 2005). Most importantly, *Q. suber* plays a crucial role in Mediterranean ecosystems by providing protection against desertification and soil erosion, which makes it a vital tree for the local economy and environmental sustainability (Pereira, 2007).

1.4.4 Insights from previous studies on selected candidate genes

Just as the vascular cambium produces secondary xylem outward, the phellogen similarly generates phellem in a centrifugal direction. Both tissues are part of secondary growth but differ in function and chemical compositions. In 2019, Lopes *et al.* aimed towards the identification of new putative molecular regulators of secondary growth specifically enriched in the phellogen/phellem through an RNA-seq comparative transcriptomic analysis of the phellogen/phellem versus xylem cells in *Q. suber* (Lopes et al., 2020). From this research, a list of differentially expressed genes between the two tissues was identified and only 4% being up-regulated exclusively in phellem and phellogen (Lopes et al., 2020). A smaller list of candidate genes was then obtained upon screening the suberization in *Arabidopsis* hypocotyls undergoing secondary growth in selected mutants (Susana Lopes, personal communication, unpublished). The list of candidate genes previously identified was further detailed through a histological analysis of the suberization patterns in the root endodermis of *Arabidopsis* seedlings (Cavaco, 2022). The candidates WUSCHEL-RELATED HOMEOBOX 9 (WOX9, also known as STIMPY), AINTEGUMENTA (ANT), and MYB36 are pointed as possibly involved in the suberin biosynthesis and deposition processes (Cavaco, 2022). WOX9 is essential in the maintenance of the stem-cell population in the apical shoot meristem, promoting cell division in the root, and is activated by cytokinin signals in the meristem (Skylar et al., 2010; Wu et al., 2005). The analysis of the suberin root coverage in loss of function mutant alleles (*stip-1* and *stip-2*) showed a decrease in the continuous suberin area, along with an increase of the patchy suberin and non-suberized areas, compared to the wild-type. Conversely, the gain-of-function mutant (*stip-D*) revealed a decrease in the non-suberized zone, suggesting that WOX9 is acting as a positive regulator of the suberization process (Cavaco, 2022). Moreover, it was shown that *stip-1* mutant has reduced expression of several genes involved in the suberin biosynthesis (Cavaco, 2022). The AINTEGUMENTA (ANT), encoding an AP2-domain transcription factor, has been reported essential in the control of plant organ size and ovule formation, as well as implicated in the regulation of root secondary growth (Elliott et al., 1996; Mizukami & Fischer, 2000; Randall et al., 2015). The loss of function allele *ant-9* showed a reduction in the extension of the continuous suberin zone and an increase in the patchy suberin, suggesting its involvement as a positive regulator of the endodermis suberization during early development (Cavaco, 2022). MYB36 is a transcription factor expressed in the endodermis that is a positive regulator of the Casparian strip formation (Kamiya et al., 2015). The loss of function *myb36-1* revealed an increase of patchy and continuous suberin zones in the root, pointing to a negative regulation of the suberization process by MYB36 (Cavaco, 2022).

1.5 Objectives

The suberization defects found in the endodermis of the candidate genes' mutants recently characterized in the laboratory (Cavaco, 2022) support an important role for these genes in suberized tissues. Therefore, the main goal of this work is to contribute to the further characterization of the identified candidates, namely *WOX9* and *ANT*. To achieve this goal, we aimed at:

1) Understanding the impact of *ANT* candidate on the suberin biosynthetic pathway, through an RT-qPCR expression approach.
2) Exploring potential interactions of the candidate genes' with ABA pathway through the study of the effect of exogenous ABA supply on *ant-9* seedlings, followed by RT-qPCR expression analysis of genes involved in this pathway on *ant-9* and *stip-1*, *stip-2* and *stip-D* mutants.

3) Building the tools for assessing functional conservation of the WOX9 candidate in Arabidopsis and *Q. suber*. Genetic constructs for functional complementation of Arabidopsis *wox9* mutants with QsWOX9 were prepared and transferred by Agrobacterium-mediated transformation to assess the possible alterations in the mutants suberization patterns.

2 Materials and Methods

2.1 Plant material and growth conditions

Arabidopsis thaliana Landsberg *erecta* (L*er*) and Columbia (Col-0) ecotypes were used in all experiments. The *ant-9* loss-of-function mutant of the *ANT* gene (AT4G37750) contains an insertion of a transposable element on the intron 2 (Elliott et al., 1996). For the study of the *WOX9* gene (AT2G33880) two loss-of-function mutant alleles were used, *stip-1* which is formed by a T-DNA insertion in the second intron, identified from the Wisconsin T-DNA collection, and *stip-2* containing a substitution that causes a missense mutation of the codon 103. Additionally, the overexpression mutant *stip-D*, with an insertion 270 bp downstream of the transcription starting site generated by activation tagging (Wu et al., 2005), was used. All the *WOX9* mutants are in Col-0 background (Wu et al., 2005).

Arabidopsis seeds were surface sterilized with 1 mL 35% commercial bleach (HClO) for 2 min with shaking, followed by 5 washes with 1 mL sterile milliQ water, and sown on Murashige and Skoog (MS) basal salt medium, supplemented with 1x MS Vitamins (Duchefa Biochemie, Netherlands), 0,8% (w/v) plant agar (Duchefa Biochemie, Netherlands), and 0.5% (w/v) Sucrose (Duchefa Biochemie, Netherlands) and pH adjusted to 5.6-5.8 interval, in square 12 cm ×12 cm Petri dishes sealed with 3MM Micropore tape. The seeds were incubated in the dark at 4ºC for 3-5 days for stratification. Then, seeds were transferred to 22ºC in darkness for 24h, after which the plants were grown vertically at 22ºC under long-day conditions (16h light and 8h dark), 60% rH.

For the ABA treatments, 'wild-type' L*er* ecotype and *ant-9* seeds were surface sterilized, sown and stratified as described above, and grown at 22ºC under long-day conditions (16h light and 8h dark), 60% rH in a climatic chamber. After 3 days of growth on MS medium, at least 10 Ler and 10 *ant-9* seedlings were transferred to MS plates supplemented with 1 µM ABA (Sigma-Aldrich, USA) and at least 10 Ler and 10 *ant-9* seedlings were transferred to mock treatment plates (MS medium), where plants were grown under the same conditions for 24h. For the complementation assays and for the expression analyses, *Arabidopsis thaliana* wild-type Col-0, the loss-of-function mutant lines *stip-1* and *stip-2*, the overexpression mutant *stip-D*, Ler and *ant-9* seeds were grown for 7-9 days in the above-described conditions. For the growth of the *stip-1* seeds, 15 µg/L Phosphinotricin (PPT) (Duchefa Biochemie, Netherlands) was added to the MS agar plates for the selection of BASTA-resistant mutant seedlings. After 7-9 days *stip-1* and Col-0 seedlings were transplanted to pots containing soil (3:1 mix of peat:vermiculite (Projar, Spain), and were grown at 22ºC under long-day conditions (16h light and 8h dark), 60% rH in a climatic chamber.

2.2 DNA and RNA extractions

"Amadia" cork samples used for total RNA extraction were previously obtained from cork oak planks freshly removed by specialized workers from cork oak trees in the period of intense phellogen activity (July 2016). The inner surface of the planks was scraped with a sterile scalpel collecting phellem cells

and phellogen cells present on the surface and samples were stored in liquid nitrogen immediately after collection and stored at -80ºC (Lopes et al., 2020). All RNA extractions from cork were performed prior to the initiation of this work (Lopes et al., 2020). Briefly, samples were ground to fine powder and homogenized in extraction buffer, at 65ºC for 5 min. Followed by two extraction steps with chloroform:isoamyl alcohol, and washed with 70%, and 100% ethanol. The dry pellet was resuspended in diethyl pyrocarbonate (DEPC)-treated water, and the RNA samples were DNase treated to ensure genomic DNA removal and quantified (Chang et al., 1993; Lopes et al., 2020).

For the expression analysis, 100 mg of each tissue (Arabidopsis root-hypocotyl, base of the stem, and leaves) were collected from 24 adult plants, and six pools of four individuals were assembled for each tissue and immediately frozen in liquid nitrogen then stored at -80ºC. From each pool, 65-100 mg of tissue was ground to fine powder and total RNA was extracted by RNeasy Plant Mini Kit (Qiagen, Germany). The RNA integrity and the efficient removal of DNA were assessed by 1% agarose gel electrophoresis to assess DNA contamination. Samples were treated with TURBO DNA-free kit™ following manufacturer's instructions (Invitrogen, USA) as described by Cavaco (2022).

2.3 Primer design and optimization

The specific primers for the amplification of Qs*WOX9* (LOC112020126; Table 2.1) were designed to amplify the coding sequence from the *Q. suber* annotated genome on CorkOakDB (http://corkoakdb.org/), using Primer3 (https://www.primer3plus.com/; Untergasser et al., 2012). The properties of each primer were analyzed on Sequence Manipulation Suite: PCR Primer Stats (https://www.bioinformatics.org/sms2/pcr_primer_stats.html), including GC percentage, melting temperatures, self-annealing and hairpin formation.

For the expression analysis, the specific primers for the selected suberin biosynthetic specific genes (*KCS2, GPAT5, ABCG6, CYP86A1, CYP86B1, ASFT, FAR1* and *GELP38* were designed based on Nomberg et al., 2022 and *ACTIN2* was used as reference gene. Primers were previously designed for the coding region of each gene using Primer3Plus (https://www.primer3plus.com/) and the properties of each primer were analyzed on Sequence Manipulation Suite: PCR Primer Stats (https://www.bioinformatics.org/sms2/pcr_primer_stats.html)(Cavaco, 2022). The specific primers used in Reverse transcription-quantitative polymerase chain reaction (RT-qPCR) to target ABA pathway-specific genes (*NCED3, PYR1, PP2CA, CYP707A1*) were designed according to Chan, 2012. A set of different annealing temperatures and extension times were tested to optimize for high-specificity primer annealing and optimal product amplification. The primers used and respective conditions of amplification, as well as primer efficiency, are shown in Table 2.2. Each polymerase chain reaction (PCR) was assembled using 1x Green GoTaq Reaction buffer, 1.5 mM MgCl2, 10 mM of dNTPs mix, 0.5 μM of each primer, and 1.25U of GoTaq DNA polymerase (Promega, USA). The reaction products were visualized in 1% Agarose gels.

Table 2.1 List of primers used for the construction of the complementation vector

Primer Name	Primer Sequence	Amplicon Size (bp)	Annealing Temperature (ºC)	Extension time (s)
QsWOX9_F	GGGGACAAGTTTGTACAAAAAAGCAGGCTCCATG GCTTCATCTAACAGACAC	1245	56	35

QsWOX9_R	GGACCACTTTGTACAAGAAAGCTGGGTCCACAAG TGCACAGGAACCAT

Table 2.2 List of primers used in the RT-qPCR analysis.

Primer Name	Primer Sequence	Annealing Temperature (ºC)	Extension Time (s)	Primer Efficiency (%)
GPAT5_F	ACCGTGTCGCTAATTTGTTTGTTGG	60	30	109
GPAT5_R	CCGTCGTGAAATATCACCGGAAGT			
KCS2_F	GCTTGAGAAAACCGGAGTGA	60	30	101
KCS2_R	GAGAAGCATTGATCGGTCGT			
FAR1_F	GGAGCCCTGAATGTTCTCAACTTCG	60	30	104
FAR1_R	GAGAGTCTCCCCCATCTTGAATGGT			
CYP86A1_F	TCGTTTACCTCAAGGCTGCT	60	30	88
CYP86A1_R	GGAGTCTCAAACCGTTCACC			
ASFT_F	TACCAAACCCGATCCTGAAA	60	30	90
ASFT_R	GCTCCAATTCCATCGAACAT			
ABCG6_F	ATGAACCAACTTCGGGTCTG	60	30	103
ABCG6_R	CGGGACAAGAAGAGAAGACG			
GELP38_F	ACGGGTTTGATAACTCGGATTCG	60	20	101
GELP38_R	ACAATGTCGACGCTGGAATACACG			
CYP86B1_F	CCCGCTGATCACAAAGAGG	60	30	101
CYP86B1_R	GAACCGTCCGTCTCTTAGCC			
ACTIN2_F	GGCTCCTCTTAACCCAAAGG	60	30	106
ACTIN2_R	TTCTCGATGGAAGAGCTGGT			
NCED3_F	AGCTCCTTACCTATGGCCAG	60	20	94
NCED3_R	CGCTCTCTGGAACAAATTCATC			
PP2CA_F	AAGATCGGTACGACGTCGGTTTGT	60.3	16	106
PP2CA_R	TCTGCACTTCTCCGCAACATGAGA			
PYR1_F	GCGAACACATCAACGGAAAG	60.3	16	97
PYR1_R	CCAGATCCGATTCTCTTTCTCG			

CYP707A1_F	AACTCAGGAAGCTTGTTCTTCG	60	16	103
CYP707A1_R	AGATCGATAGCAACGCAACG			

2.4 cDNA synthesis and RT-qPCR

The first strand complementary DNA (cDNA) was synthesized from 1 µg of previously extracted and DNase-treated Arabidopsis *ant-9* and L*er* total RNA, using the Thermo Scientific Revert Aid First Strand cDNA Synthesis Kit #K1621 (Thermo Fisher Scientific, EUA) following the manufacturer's directions. The diluted (1:10) cDNA was used for the quantitative PCR analysis. Each reaction was set up for 10 µL final volume containing 5 µL 1X SsoAdvanced Universal SYBR Green Supermix (Bio-Rad, EUA), 500 nM of each primer, and 1.5 µL of diluted cDNA) on optical 96-well BR White plates and (Bio-Rad, EUA). Three biological replicates were used for each amplification reaction, with technical triplicates of each cDNA sample, and a pool of 3 wild-type root-hypocotyls cDNA was used as positive control.

To determine the amplification efficiency of each primer pair, a standard curve was constructed using serial dilutions of (1:20; 1:50; 1:100; 1:200; 1:500; 1:1000) of the cDNA template. The amplification reactions were performed on a CFX96 Touch Real-Time PCR Detection System (Bio-Rad, EUA) in the following conditions: initial denaturation step at 95ºC for 3 min followed by 40 cycles, each consisting of a denaturation step at 95ºC for 10s, followed by an annealing/extension step at 60ºC for 30s (for *GPAT5, KCS2, FAR1, CYP86A1, ASFT, ABCG6, ACTIN, CYP86B1*), 60ºC for 20s for *GELP38* and *NCED3*, 60ºC for 16s for *CYP707A1* and 60.3 ºC for 16s for *PP2CA* and *PYR1*. Afterwards, a final melt-curve step, at 65-95ºC in 0.5ºC increments for 2-5 seconds, confirmed the presence of a single PCR product. The same amplification conditions were used for the sample amplification. The primer efficiency was calculated from the standard curve by:

$$Efficiency\ (E) = 10^{-\frac{1}{Slope}}$$

Which can be converted to percentage by

$$\%\ Efficiency = (E - 1) \times 100$$

Relative expression values for each target transcript were calculated according to (Pfaffl, 2001) to consider the different amplification efficiencies between the genes of interest (target gene) and the reference gene *ACTIN2* in the ratio to determine the relative transcript, using the formula:

$$Ratio = \frac{(E_{target})^{\Delta C_{t,target}(control-sample)}}{(E_{ref})^{\Delta C_{t,ref}(control-sample)}}$$

2.5 Whole-mount suberin histological staining after hormone treatment

The lipophilic Fluorol Yellow 088 (FY, ChemCruz, EUA) stain was used to study the effect of exogenous ABA supply on the root endodermis' suberization patterns in the suberized cell walls of *ant* loss of function mutant (Barberon et al., 2016; Brundrett et al., 1991; Lux et al., 2005; Naseer et al., 2012). Seedlings were grown vertically on MS medium for 3 days after germination and harvested to

customized histological cassettes sealed with 3MM Micropore tape. Seedlings were then incubated in freshly prepared FY (0.01% w/v, in lactic acid), pre-heated at 70ºC for 10 min in a lab oven (ThermoFisher Scientific, USA), in darkness for 30 min followed by 3 consecutive 5 min washes with room temperature sterile water to remove accumulated FY precipitates on the surface of the root. Seedlings were submerged in room temperature Aniline Blue (AB) (0.5% w/v in water, Duchefa Biochemie, Netherlands) solution, for counterstaining, for 15 min in darkness and the remaining AB on the root surface was removed by 4 washes of 7 min in room temperature sterile water. Seedlings were kept in darkness throughout the protocol. To ensure tissue preservation during slide preparation the seedlings were transferred to 25% glycerol (Carl Roth, Germany), mounted on glass slides in 30-50 µL of Antifade mounting medium (1 part of 10x Phosphate Buffered Saline (PBS) in 9 parts of Glycerol (Merck KGaA, Germany) with 0.5% (w/v) n-propyl gallate (Sigma-Aldrich, USA) in dimethyl formamide (Sigma-Aldrich, USA) to delay the photobleaching effect on the fluorochrome signal during observation, using tweezers to position the root as linear as possible, and covered with a slide coverslip (Cavaco, 2022). Stained seedlings were imaged within 4h after the preparation of the samples to avoid fluorescent signal leaking into the xylem. This procedure was performed for the 4-day-old seedlings on 24h ABA or mock treatment.

2.6 Microscopy

Confocal laser scanning microscopy imaging was performed on a Leica TCS SPE based on a Leica DMI4000B (Leica, Germany). The excitation and detection windows for FY staining were 488 nm and 500-550 nm. All observations used a 10x objective magnification. A tile scan function was used to obtain a mosaic of the seedling full length and a z-stack function of 15 images 10 nm along a 150 nm z length was used to produce a maximum projection in Leica Application Suite X (Leica, Germany).

2.7 Root suberin coverage assessment

For the analysis of suberization patterns, the regions from the tip of the root to the root-hypocotyl junction were assessed and categorized as follows. The distance measured from the tip of the root until the first suberized endodermal cell appears determines the ‘non-suberized region’, the distance from that first suberized cell until measured to the hypocotyl corresponds to the ‘suberized’ region. The sum of the two zones is the total root length (Andersen et al., 2021; Barberon et al., 2016; Cavaco, 2022).

2.8 Molecular cloning

To generate expression constructs for the complementation of Arabidopsis mutants with *Q. suber WOX9 (QsWOX9)*, the first strand complementary DNA (cDNA) was synthesized from 1µg of previously extracted and DNase-treated *Q. suber* total RNA, using the Thermo Scientific Revert Aid First Strand cDNA Synthesis Kit #K1621 (Thermo Fisher Scientific, EUA). Specific primers were used to amplify the QsWOX9 coding sequence (CDS) (Table 2.1 from the cDNA template in a PCR reaction using 1× Phusion GC Buffer, 10 mM of dNTP mix, 1 mM MgCl2, 0.5 µM of each primer, Phusion High-Fidelity DNA Polymerase.

In a thermocycler, the following conditions were applied for the reaction: initial denaturation at 98ºC for 30s, followed by 35 cycles of a denaturation step of 10s at 98ºC followed by a 30s annealing step at 70ºC, extension of 35s at 72ºC, and a final extension step at 72ºC for 10 minutes. The amplification

products were visualized in 0.8% ultra-pure agarose gels and purified from the agarose band cut from the gel, following the High Pure PCR Product Purification Kit (Roche, Switzerland) manufacturer's instructions, and the PCR products were eluted in 30 µL of (DEPC)-treated water. The PCR product's concentration and purity were evaluated using a NanoDrop-1000 spectrophotometer (Nanodrop Technologies Inc., USA). The *QsWOX9* CDS was first cloned into a pDONR221 Gateway vector using BP Clonase II Enzyme Mix (Invitrogen, USA) according to the manufacturer's directions. The pENTRY plasmid generated was transformed into 25 µL of chemically competent *E. coli* Top 10 strain (Thermo Fisher Scientific, EUA) by incubating the competent cells with the plasmid for 30 min on ice, followed by 30s in a 42ºC bath, and placed on ice, after which 250 µL of SOC medium was added. The cells grew for 3h at 37ºC, 200 rpm, and were then spread on LB agar plates supplemented with 50 $\mu g \cdot mL^{-1}$ of Kanamycin for selection of transformed colonies. The plates were incubated at 37ºC overnight. Once colonies were formed, a colony PCR was performed using the GoTaq polymerase (reaction assembled as follows: 1× Green GoTaq Reaction buffer, 1.5 mM MgCl2, 10 mM of dNTPs mix, 0.5 µM of each primer, and 1.25U of GoTaq DNA polymerase (Promega, USA)) using M13 universal primers. To confirm the transformed status of the cells, the products were visualized in 1% Agarose gel. The colonies amplifying the expected product size were selected and grown overnight in liquid LB medium supplemented with 50 $\mu g \cdot mL^{-1}$ of Kanamycin. The plasmid was extracted using the GeneJet Plasmid Miniprep Kit (Thermo Fisher Scientific, EUA) according to the manufacturer's instructions. To confirm the integrity of the sequence cloned, the DNA sequences were analyzed by Sanger sequencing using M13 universal primers.

The plasmid with the least number of mismatches was selected to recombine with a pK7WG2 Gateway destination vector, which contains the 35S promoter from Cauliflower Mosaic Virus (CaMV) using LR clonase II (Invitrogen, USA) reaction, following the manufacturer's description, to generate the 35S::*QsWOX9* construct. The generated plasmid was transformed into 50 µL of chemically competent *E. coli* DH5α (Thermo Fisher Scientific, EUA) by incubating the competent cells with the plasmid for 30 min on ice, followed by 30s at 42ºC bath, and placed on ice for 2 min, after which 250 µL of SOC medium was added. The cells grew for 3h at 37ºC, 200 rpm, and were then spread on LB agar plates supplemented with 50 $\mu g \cdot mL^{-1}$ of Spectinomycin for selection of transformed colonies. The colonies were tested by colony PCR as above described.

2.9 *Agrobacterium tumefaciens*-mediated Arabidopsis transformation

2.9.1 Preparation of bacteria competent cells and transformation

The *A. tumefaciens* LBA4404 was grown, from a pre-existing stock, in 5 mL of liquid LB medium supplemented with Rifampicin 50 $\mu g \cdot mL^{-1}$, to select the bacteria, and grown overnight at 28ºC at 200 rpm. 2 mL of the overnight culture was transferred to 50 mL liquid LB with Rifampicin 50 $\mu g \cdot mL^{-1}$ and incubated at 28ºC at 200rpm until the culture achieved OD_{600} 0.5-1.0. Once the desired OD_{600} was achieved the cell culture was placed on ice and centrifuged at 3000×g for 5 min at 4ºC. The supernatant was discarded and the cells were resuspended in 1 mL of 20 mM $CaCl_2$ solution at 4ºC, distributed in 100 µL aliquots in 2 mL microtubes, and immediately frozen in liquid nitrogen and stored at -80ºC.

To transform the competent *A. tumefaciens* LBA4404 with the p35S::*QsWOX9*, first 545 ng of plasmid was added to the 100 µL of frozen competent cells, followed by a 5 min incubation at 37ºC in a water bath to thaw the cells, after which the cells were incubated on ice for 30 min. Finally, the cells were

spread on LB agar plates supplemented with 50 μg·mL^{-1} Rifampicin and 50 μg·mL^{-1} Spectinomycin to select the transformed bacteria, and incubated at 28ºC for at least 2 days. The resulting colonies were tested by PCR using *QsWOX9*-specific primers. The amplification products were observed in an electrophoresis 1% agarose gel.

2.9.2 Arabidopsis floral dip transformation

To prepare the *A. tumefaciens* suspension for plant transformation, a single colony (previously tested positive) was inoculated into 5 mL of LB medium supplemented with 50 μg·mL^{-1} Rifampicin and 50 μg·mL^{-1} Spectinomycin and incubated at 28ºC for 24h-48h at 220 rpm. 5mL of the preculture was transferred to 500 mL of LB supplemented with the selective antibiotics and grown overnight at 28ºC at 200 rpm. The OD_{600} was measured and once OD_{600} ~1 was reached the bacteria were centrifuged for 10 min at 4 000×g) and the pellet was resuspended in 500 mL of a freshly made solution of 5% sucrose, 10 mM $MgCl_2$ and 0.05% (v/v) Silwet L-77.

Three months old Col-0 and *stip-1* plants with numerous inflorescences containing young flowers as well as some unopened floral buds were transformed using the floral dip method (Clough & Bent, 1998). Watering of the plants was removed 4 days before the transformation day and all the already formed siliques were removed. The inflorescences were dipped in the bacterial suspension for 15 seconds with gentle agitation. Afterwards, each pot was labelled, wrapped in Saran Wrap to maintain humidity and laid on its sides overnight, in darkness. Afterwards, the plants were unwrapped and positioned upwards in standard growth conditions and normal watering regimen. The process was repeated after 8 days to increase transformation rates (Clough & Bent, 1998). When the seeds became mature the first siliques were harvested and watering ceased when most siliques appeared mature.

2.10 Data analysis

GraphPad Prism software (version 9.0.0) (www.graphpad.com) was used for the statistical analysis of the relative expression values and the suberin root coverage values. The sample groups were analyzed with parametric T-student tests (p-value <0.05) to infer significant differences and plotted accordingly using the same software.

3 Results

3.1 WOX9 affects ABA signaling

Preliminary studies conducted in our lab showed that *WOX9/STIP* might be a positive regulator of endodermis/periderm suberization in Arabidopsis. The exogenous supply of ABA partially restores the suberization in the loss of function *stip-1* endodermis, increasing the suberized zones in the root of seedlings treated with ABA, indicating *WOX9* might act upstream the ABA biosynthetic or signaling pathways in the suberization process (Cavaco, 2022). To test whether *WOX9* affects the ABA pathway we measured the transcript levels of key genes of the ABA biosynthetic, signaling and catabolic pathways in gain and loss of WOX9 function genetic backgrounds. To understand whether the alterations in the endodermis suberization in mutant alleles of *WOX9* were the result of affected ABA biosynthesis, we measured the transcript levels of the 9-CIS EPOXY CAROTENOID DIOXYGENASE 3 (*NCED3*) which encodes a key enzyme of the ABA biosynthesis (Iuchi et al., 2001; Tan et al., 2003).

In root and hypocotyl tissues, no significant differences were found in the slightly reduced *NCED3* transcriptional levels of *stip-1* loss of function mutant, relative to the wild-type (Figure 3.1).

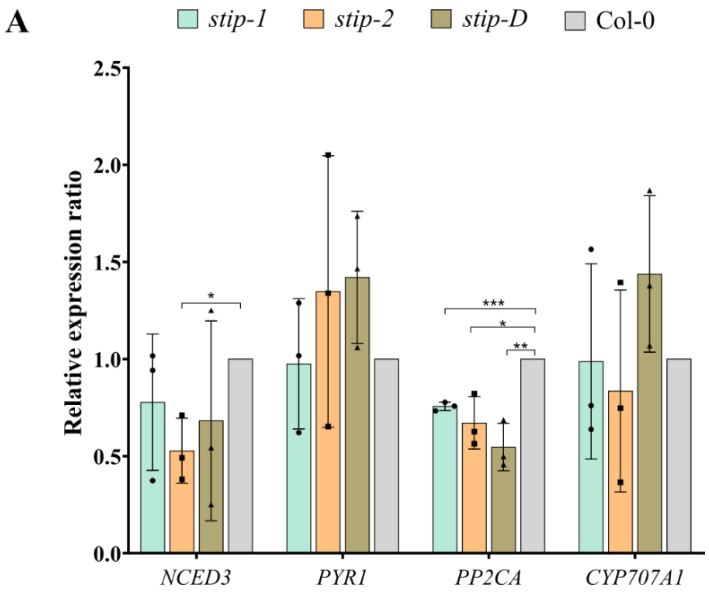

Figure 3.1 Abscisic acid pathway gene expression is affected in *WOX9/STIMPY* mutants. mRNA steady state transcript levels of NCED3, PYR1, PP2CA and CYP707A1 were measured by quantitative real time PCR to root-hypocotyl tissues of 3-month-old loss-of-function mutants, *stip-1* and *stip-2*, the overexpression *stip-D*, and wild-type Col-0 plants. *ACTIN2* was used as reference gene. Statistical significance between mutants and wild-type using an unpaired *t*-test is represented by ***p<0.001, **p<0.01, *p<0.05. (n=3)

The weak loss-of-function allele *stip-2*, however, revealed a significant (p = 0.008) decrease in the *NCED3* expression levels relative to the wild-type, indicating that *WOX9* absence might have a negative effect on the ABA biosynthesis. The transcriptional levels of the PYRABACTIN RESISTANCE 1 (*PYR1*), which is part of the PYR/PYL/RCAR ABA receptors family and a positive regulator of the ABA signaling (Park et al., 2009), were measured to study whether the ABA signaling pathway was affected in the root-hypocotyl tissues. The transcript levels of the *PYR1*, revealed no significant differences between the WT and *stip-1* or *stip-2* (Figure 3.1). Despite no significant differences observed in the expression levels of *PYR1* in the *stip-D* overexpression mutant, there was a slight increase in *PYR1* expression that suggests an increase of ABA perception machinery coinciding with increased suberization. Supporting this view, the transcriptional levels of the PHOSPHATASE TYPE 2C belonging to clade A (*PP2CA*) a negative regulator of the ABA signaling pathway inhibited by PYR1 in an ABA-dependent manner (Kuhn et al., 2006; Yoshida et al., 2006) were reduced in both loss of function *stip-1* and *stip-2* alleles, and especially reduced in the overexpression *stip-D mutant* (Figure 3.1). These results indicate an interaction of WOX9 with the ABA pathway impacting the ABA signaling, suggesting operation of a regulatory mechanism controlling suberization via ABA signaling involving *WOX9*, in a way that the overexpression of *WOX9* would induce intracellular ABA receptors PYR1 expression which on its turn inhibit the ABA negative regulator *PP2CA* expression. Overall, this might result in the increased ABA signaling cascade and increased ABA response through suberization in the endodermis, an effect previously observed in *stip-D* (Cavaco, 2022). Consistent with this hypothesis is the increase in the catabolic *CYP707A1* expression in *stip-D (*Figure 3.1). The *CYP707A* from the cytochrome P450 monooxygenase family plays an important regulatory role in controlling ABA levels in plants (Kushiro et al., 2004). The increase in suberization observed in *stip-D* hypocotyl

periderm and root endodermis might be the result of *WOX9* directly or indirectly being involved in the control of intracellular ABA signaling and levels.

3.2 *stip-1* mutant complementation with cork oak *WOX9*

Considering the impact of *WOX9* on the suberin deposition, with delayed endoderm suberization in both *stip-1* and *stip-2* loss of function mutants during early development(Cavaco, 2022), we wondered whether *WOX9* has a conserved function between Arabidopsis and cork oak where it was initially indicated as involved in the cork formation process (Lopes et al., 2020). We used Protein BLAST (Altschul et al., 1997) to conduct the protein sequence alignment comparing the sequences of Arabidopsis *WOX9* to that of QsWOX9, which revealed a 47% identity between the sequences (Figure 3.2 A).

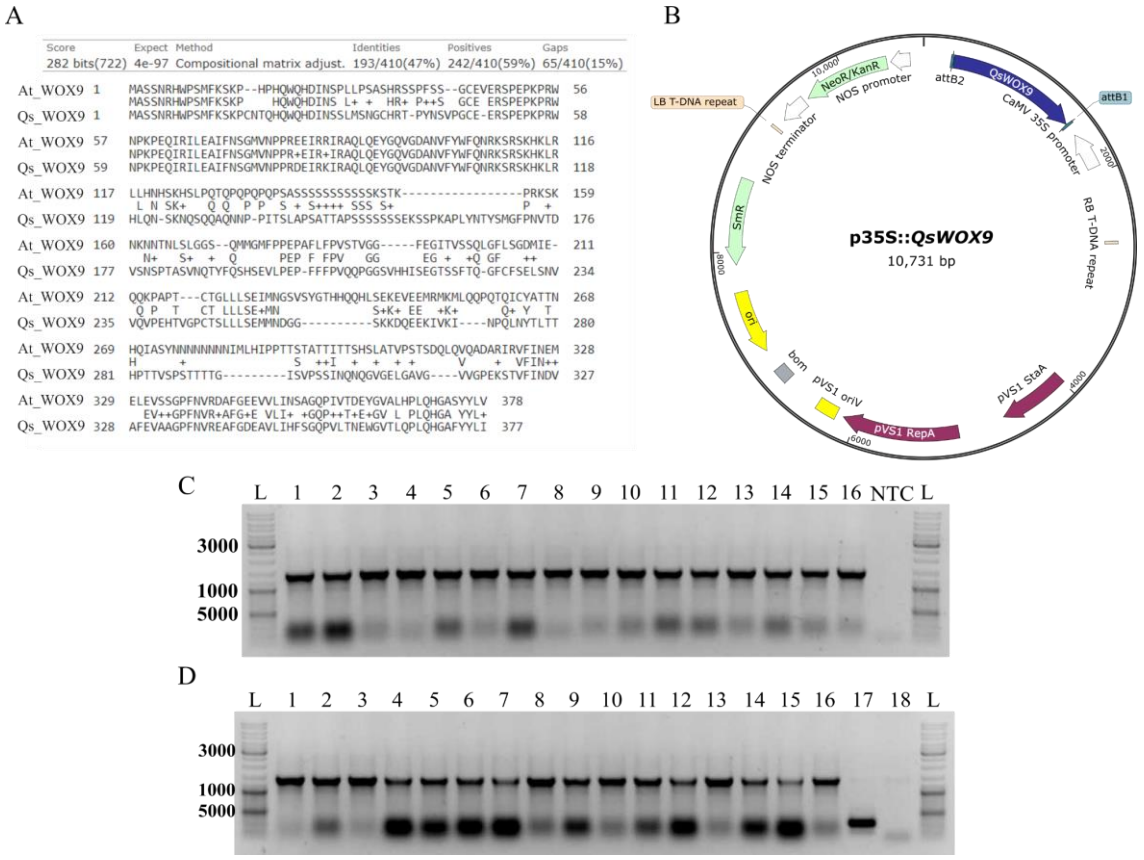

Figure 3.2 Isolation of QsWOX9 and plasmid construction. (A) The sequences of Arabidopsis WOX9 and QsWOX9 translated proteins were compared using the BLAST tool. (B) Expression vector p35S::QsWOX9 resulting from the cloning of QsWOX9 into the pK7WG2 plasmid (map constructed using SnapGene software). (C and D) Electrophoresis gel results showing the QsWOX9 successfully isolated in pDONR221. The gels show the colony PCR using universal M13 primers in which all colonies (numbers) present amplification between the marked 1200-1500 bp, corresponding to the expected amplicon size of 1480 bp. L – GeneRuler DNA ladder Mix (ThermoFisher Scientific, USA), NTC- non-template control, 17 - negative contro, 18 - pDONR221 without the ccdB cassette.

In order to investigate whether the two proteins have a conserved function we conducted a cross-species complementation experiment in the loss of function allele *stip-1*, in Arabidopsis. To this purpose, the coding sequence of cork oak *WOX9* (QsWOX9) was obtained from CorkOakDB (http://corkoakdb.org/) and specific primers adapted for Gateway cloning technology were designed for amplification of this region (Tabel 2.1). The *QsWOX9* CDS was successfully isolated from cDNA, derived from "Amadia"

cork samples, in an entry vector (pDONR221), confirmed by PCR of *E. coli* colonies transformed with the entry vector containing *QsWOX9* CDS (Figure 3.2. C, D). This vector was then recombined with the pK7WG2 binary vector containing a 35S promoter (Figure 3.2 B), containing the plant kanamycin selectable marker. Flowers of Arabidopsis 'wild-type' and *stip-1* mutant allele were transformed by the floral dipping method, with Agrobacterium harboring the 35S::*QsWOX9* construct. We are currently retrieving transformed seeds that will be screened using the plant selectable marker (kanamycin resistance) to identify the transformed seeds, which will then be stained with FY for the characterization of the seedling root endodermis suberization patterns.

3.3 ANT might be a positive regulator of endodermis development/suberization

The transcription factor ANT plays a key role in the regulation of genes implicated in floral organ initiation, growth and identity in Arabidopsis (Elliott et al., 1996; Krizek, 2009), and was identified as a putative candidate involved in the cork formation process in cork oak (Lopes et al., 2020). We analyzed the endodermis suberization in the *ant-9* loss-of-function mutant. Cavaco (2022) reported an increase in the 'non-suberized' and 'patchy' zones and a reduction of the 'continuous' suberized zone of the 7-day old *ant-9* root. To understand if the suberization was delayed earlier during endodermis development, we investigated the pattern of root suberization in younger seedlings of *ant-9* and in the wild-type L*er*, the background in which the mutation was identified (Elliott et al., 1996). To this end, we used Fluorol Yellow 088 (FY), which specifically stains the suberin lamellae, to stain the roots of seedlings 3 days after germination (dag), and observed the suberized endodermal cells under the better resolution of a confocal microscope, assessing the total extension of 'non-suberized' and 'suberized' zones of the root (Barberon et al., 2016; Lux et al., 2005). Surprisingly, we did not observe a significant difference when comparing the loss-of-function *ant-9* with the L*er* (wild-type), as Cavaco (2022) reported. This shows that the reduced suberization observed in *ant-9* at 7 dag does not begin as early as 3 dag, suggesting the entrance in the patchy stage of suberization is not affected by the lack of ANT and *ant-9* delay in the continuous suberization of the endodermis and periderm occurs later in development. Thus, *ANT* might operate as an enhancer of the suberization timing by speeding the entrance into the continuous stage of suberization in the endodermis.

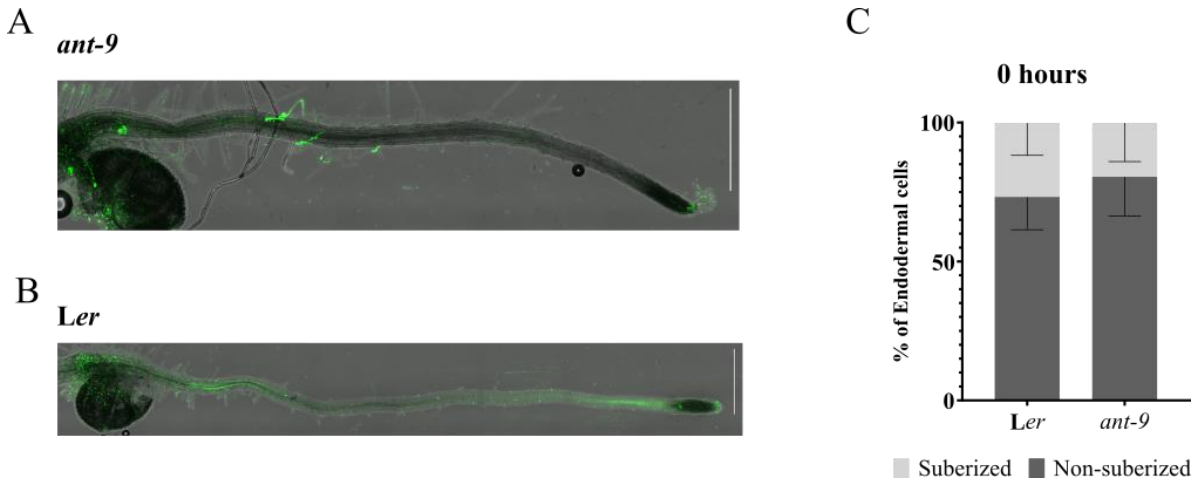

Figure 3.3 Comparison of the root suberization in the loss-of-function *ant-9* allele and wild-type L*er*. Roots of 3-day-old seedlings of *ant-9* (A) mutants and L*er* (B) were stained with FY and obseved under confocal microscopy. The root suberization coverage was calculated considering the linear distance of the 'non-suberized' areas comprised between the root tip and the first endodermal cell with detected FY signal, and the 'suberized' length corresponds to the distance between the first suberized

endodermal cell and the hypocotyl (*ant-9* n=5, L*er* n= 10). Statistical significance between treatments was calculated using an unpaired t-test and is represented by ***p<0.001, **p<0.01, *p<0.05.

3.4 ANT affects suberin-related genes expression

Suberization differences identified in the microscopy analyses reported a delay in the suberization of *ant-9* loss-of-function endodermis when compared to the L*er*. Here we sought to investigate whether the expression of key genes involved in the suberin biosynthesis and deposition pathways were affected by lack of ANT activity. To this end, we synthesized cDNA from RNA samples, isolated prior to the initiation of this work, from 2-months-old *ant-9* and wild-type L*er*, of root-hypocotyl and stem tissues, and evaluated the transcriptional levels of key genes involved in the biosynthesis of the aliphatic suberin components (*GPAT5, KCS2, FAR1, CYP86A1, CYP86B1*), conjugation of aliphatic and phenolic components (*ASFT*), transmembrane transport (*ABCG6*) and apoplastic polymerization (*GELP38*) (Figure 3.4). When we analyzed the expression of these genes in the root-hypocotyl samples, where suberization occurs (Wunderling et al., 2018), we found a decrease in the levels of the ASFT (Figure 3.4 A), which encodes a transferase that establishes the linkage between the phenolic and aliphatic suberin monomers, indicating an effect of *ANT* on the suberin assembly (Molina et al., 2009). We also found an impact on the *CYP86B1* revealing increased transcript levels relative to the wild-type, suggesting *ANT* might be involved in the regulation of the synthesis of aliphatic suberin monomers (Compagnon et al., 2009). On the other hand, in the assessment of the transcriptional levels of the same genes in stem samples, we observed reduced expression levels of most steps of the suberization mechanism (Figure 3.4 B). Those results are agreement with the absence of periderm formation and suberin deposition in the stem of Arabidopsis (Wunderling et al., 2018). Overall, the significant decrease in *ASFT* transcription levels (p-value =0.003) and the increase in the transcription levels of *CYP86B1* (p-value= 0.008) suggest a regulation of the suberin biosynthesis by *ANT*, affecting the suberin assembly, and regulating the synthesis of the very long chain of hydroxyacids.

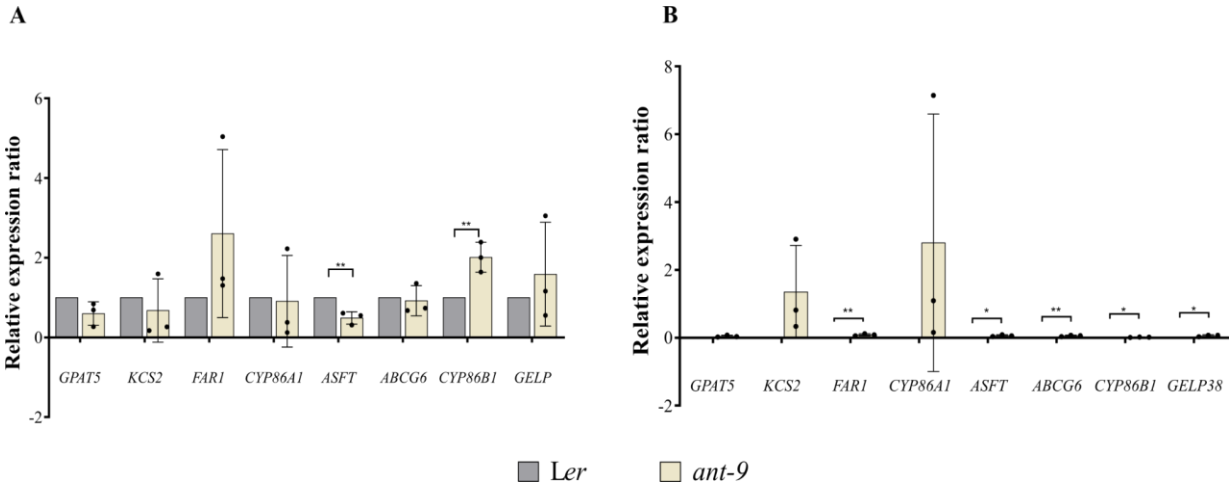

Figure 3.4 ANT affects the expression of suberin biosynthetic genes. Relative expression of suberin pathway genes in root-hypocotyl and stem of *ant-9* and L*er*. The transcript levels of the selected genes were measured by quantitative real time PCR. (A) Expression of suberin biosynthetic genes in root-hypocotyl tissues. (B) Expression of suberin biosynthetic genes in the stem tissues. The *ACTIN2* reference gene was used to calculate the relative expression. Statistical significance between each mutant and the wild-type (L*er*) was calculated using unpaired t-test and is represented by ***p<0.001, **p<0.01, *p<0.5. (n=3, each biological replicate is the pool of 4 individuals)

3.5 ABA partially reverts *ant-9* phenotype

During the endodermis development, endodermal cells undergo a secondary differentiation stage characterized by the deposition of suberin in the cell wall, contributing to the endodermis function as a diffusion barrier in roots. The plasticity shown by the endodermis in response to environmental cues relies on the ABA pathway operation, which induces the suberization of the endodermis (Barberon et al., 2016). Considering the suberization defects described by Cavaco (2022) in the *ant-9* mutant primary root suberization, we sought to investigate in a preliminary experiment, whether the suberization defects reported result from an effect of the ANT loss-of-function on the ABA signaling pathway and whether ABA-induced suberization is affected. Therefore, 3-days-old *ant-9* and L*er* seedlings were transferred to growth medium supplemented with 1 µM of ABA, and grew in ABA for 24h. This concentration was chosen since it has no greater effects on other aspects of root development (Barberon et al., 2016). As expected, the 4-day old wild-type L*er* seedlings exposed to 1µM ABA treatment revealed a steep increase in the FY-stained suberized zone (32.30 ± 8.836%) when compared to the seedlings maintained in the mock treatment (p = 0.008) (Figure 3.5).

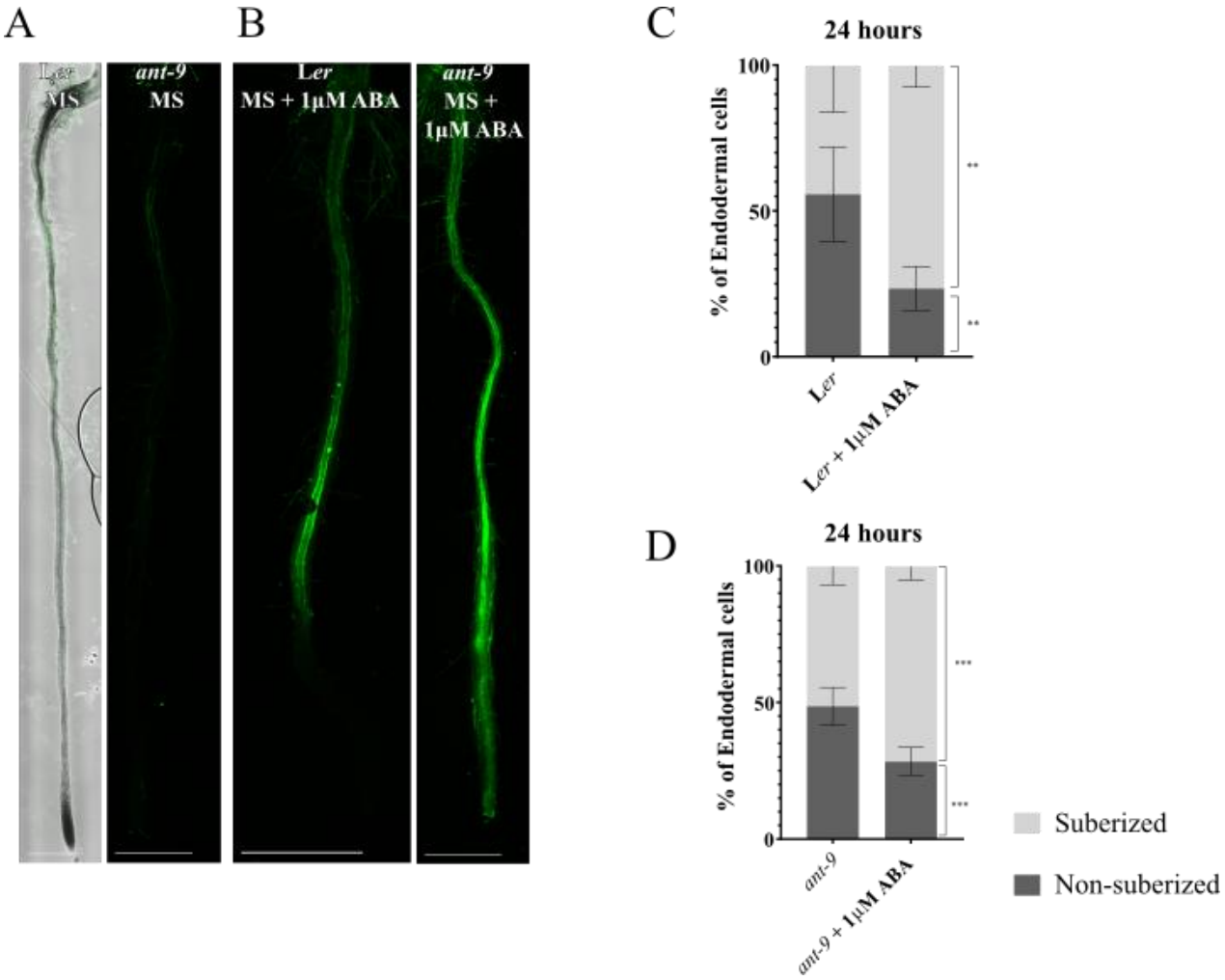

Figure 3.5 Effect of exogenous ABA supply on *ant-9* mutant and wild-type L*er*. 3-day-old *ant-9* and L*er* seedlings we treated with ABA for 24h**,** stained with FY and observed under confocal microcopy. the alterations in root suberization pattern were evaluated in relation to the seedlings at the same developmental time on control (mock) treatment. (C) The percentage of non-suberized and suberized and non-suberized endodermal cells on wild-type L*er* on control treatment and ABA treatment.

(D) Percentage of non-suberized and suberized on *ant-9* in control treatment and 24h ABA treatment. The suberization root coverage was determined considering the linear distance between the root tip and the first suberized endodermal cell, the distance between the first suberized cell and the region and the hypocotyl is defined as 'suberized', the sum of the two distances corresponds to the full root length (4< n <10). Statistical significance between treatments was calculated using an unpaired t-test and is represented by ***p<0.001, **p<0.01, *p<0.05.

These results show the already reported ABA-induced earlier entrance in the patchy suberization stage of the endodermis when seedlings are subjected to ABA. The FY stain in *ant-9* seedlings exposed to ABA revealed an increase of about 20% (20.23 ± 3.579 %) in the suberized zone of the roots, when compared to the mock treated (Figure 3.5). However, *ant-9* and L*er* within either treatment maintained similar suberization patters. These preliminary results show that the suberization in *ant-9* can still be induced by exogenous ABA supply, therefore suggesting that *ANT* might be acting upstream of the ABA pathway, perhaps even regulating ABA levels during the suberization process. Considering the extension and structure of the root suberization pattern observed in *ant-9* when treated with ABA, the increase in the suberized zone was concomitant with the increase in continuous suberization (not measured; Figure 3.5 B), which is a phenotype closer to the observed in the wild-type L*er* on mock treatment. Thus, ABA seems to be able to not only induce suberization in the roots of *ant-9* mutant seedlings, but also at least partially revert the mutant phenotype into wild-type.

3.6 *ANT* might be a regulator of ABA biosynthesis

Since exogenous ABA supply seems to be able to partially restore the suberization in *ant-9* loss-of-function mutants, we aimed to understand whether the ABA pathway was affected by the lack of a functional *AINTEGUMENTA*. Thus, we synthesized cDNA from RNA samples isolated from 2-months-old root-hypocotyl of *ant-9* and wild-type L*er*, and similarly to described above (section 3.1) we assessed the expression of genes in key steps of the ABA pathway: *NCED3*, *PP2CA*, *PYR1* and *CYP707A1* (Kuhn et al., 2006; Kushiro et al., 2004; Park et al., 2009; Tan et al., 2003; Yoshida et al., 2006) (Figure 3.6). We found a reduction in the relative expression of *NCED3*, which is involved in the considered rate-limiting step of the ABA biosynthesis (Iuchi et al., 2001). Conversely, no significant differences were found in the relative expression levels of *PYR1* and *CYP707A1* in *ant-9*. Additionally, a reduction in the transcriptional levels of the *PP2CA* was detected in *ant-9*. Collectively these results suggest *ANT* affects the ABA biosynthetic mechanism and might be contributing to the negative regulation of the ABA response through positive regulation of *PP2CA*.

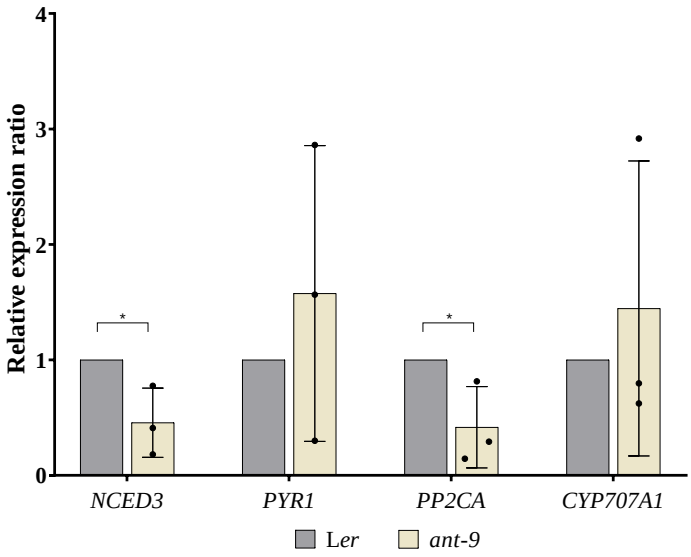

Figure 3.6 Relative expression of the genes *NCED3, PYR1, PP2CA, CYP707A1* on *ant-9* relative to wild-type L*er*. The expression analysis by RT-qPCR was performed on cDNA synthetized from total RNA extracted from root-hypocotyl tissues of *ant-9* and L*er*. All plant material and RNA extractions were performed prior to the initiation of this work. Each gene of interest was normalized with the housekeeping gene ACTIN2, and the expression ration was calculated according to Pfaflle 2001. Statistical significance between each mutant and the wild-type was calculated using an unpaired t-test and is represented by ***p<0.001, **p<0.01, *p<0.05. (n=3).

4 Discussion

The highly suberized cork layer is one of the remarkable features responsible for its high value (Pereira, 2007). Here we contribute to the characterization of two genes involved in the suberization during the early stages of development, that were identified by previous works in our lab through transcriptomics on the phellem and phellogen cells of cork oak, and histochemical studies in Arabidopsis (Cavaco, 2022; Lopes et al., 2020). We characterized the transcription factor WOX9, member of the WUS homeobox family, its effect on the ABA pathway, and investigated the impact of ANT, an AP2/ERF transcription factor, on the suberin and ABA pathways (Krizek, 2009; Mizukami & Fischer, 2000; Wu et al., 2005).

4.1 *WOX9* affects ABA signaling

The expression analysis of the ABA pathway genes in the hypocotyls of *WOX9* overexpression *stip-D* mutant shows an overall increase in the ABA signaling. This effect was found associated with the slight increase in ABA perception, as observed by enhanced *PYR1* expression, with simultaneous reduction in the expression of the ABA negative regulator *PP2CA* and an increase of the ABA catabolism (*CYP707A1*). The increase in ABA signaling could be linked to the increase in suberization in *stip-D*, since ABA is able to induce suberization even under non-stress conditions (Barberon et al., 2016). These results are consistent with the increase in suberization observed in *stip-D* roots and hypocotyls, which agrees with the hypothesis that *WOX9* might act as a positive regulator of the ABA pathway (Cavaco, 2022). Curiously, there seems to be a tight feedback system of regulation of ABA on suberization in these tissues, where increased ABA signaling is followed by an increase in ABA catabolism, showing the importance of controlling the suberization process during endodermis and periderm development.

Expression analyses to *stip-1* and *stip-2* mutants revealed a slight negative effect of the loss of *WOX9* function on the biosynthetic step of ABA pathway (*NCED3*), more significant in the phenotypically weaker *stip-2*, with no apparent significant impact on the ABA perception (*PYR1*) or catabolism (*CPY707A1*) but associated to a significant decrease in the expression of *PP2CA* negative regulator of the ABA signaling. The reduction in *NCED3* transcript suggests a reduction in the ABA biosynthesis, leading to a decrease in ABA accumulation (Sato et al., 2018). Similarly, to *stip-D*, the loss-of-function mutants display a decrease of relative expression in the *PP2CA, which* seems to suggest an increase in ABA sensitivity. However, the members of the clade A subfamily of phosphatases PP2C are known for presenting partially overlapping functions which might be maintaining the negative regulation of the pathway (Krzywińska et al., 2016; Park et al., 2009; Yoshida et al., 2006). Previous work suggests that the exogenous supply of ABA induced the suberization of *stip-1* root endodermis, indicating that *WOX9* acts upstream of the pathway (Cavaco, 2022). Indeed, the results of the present study support the hypothesis of *WOX9* functioning as a regulator of suberization through positive regulation of the ABA pathway, more specifically through its possible effect on biosynthesis and signaling.

Having established the relevance of *WOX9* for suberization of tissues in Arabidopsis, we wanted to return to the main purpose of the studies and analyze whether the function in suberization is conserved between Arabidopsis and cork oak. For that, we successfully isolated the *QsWOX9* coding sequence from cDNA, which was cloned into a destination vector building the genetic construct p35S::*QsWOX9*. The expression of *QsWOX9* under the control of the strong constitutive promoter 35S was favored over the choice of the endogenous *WOX9* promoter due to several anticipated issues followed by multiple unsuccessful attempts to clone the endogenous promoter. Additionally, p35S::*QsWOX9* is expected to ensure high transcriptional levels of *QsWOX9*, with some variation between different plant organs (Kiselev et al., 2021). Therefore, this genetic construct provides a tool for the investigation of functional similarities between QsWOX9 and the Arabidopsis homolog. The aminoacid sequence comparison between the two proteins revealed some similarity, which suggests a similar function, however, a previous motif analysis developed in our lab on WOX9 found no correspondence between WOX9 motifs and QsWOX9 questioning the functional similarity of the homologs (Cavaco, 2022). The transformed seeds produced in the first generation, by transformed *stip-1* and col-0 plants, will be analyzed by FY to characterize the suberization pattern of the seedlings, which is possible because of *stip-1* mutation, for a preliminary evaluation to the phenotype (Wu et al., 2005). We hypothesize that if the two proteins have at least partially similar functions, it is expected to observe a partial rescue of the suberization delay in the *stip-1* transformed with p35::*QsWOX9* when compared to the *stip-1*.

4.2 *ANT* affects suberin biosynthesis

The transcription factor ANT from the AP2/ERF family, is mostly known for being involved in various processes associated with floral organ and ovule development (Elliott et al., 1996; Kim et al., 2006), but also seems to play a role during organogenesis in maintaining the meristematic competence of cells (Mizukami & Fischer, 2000) and is required for proper secondary growth in the roots (Randall et al., 2015). Additionally, *ANT* has been suggested to be involved in the suberization process due to the suberization delay observed in the *ant-9* loss-of-function relative to the ‘wild-type’ L*er* (Cavaco, 2022; Lopes et al., 2020).

We have shown here that 3 days after germination the *ant-9* seedlings have a similar proportion of suberized tissue in the root to L*er* 'wild-type' seedlings. The absence of the suberization delay on *ant-9*

can be explained by the earlier stages of development observed here (3 days). Since the previous findings were observed staining older seedlings (7 days) it is possible that *ANT* operates in suberization at later stages of development than the one selected for this study. Moreover, we chose to evaluate the root suberized zones in two areas, a 'suberized' and a 'non-suberized' considering it would improve the interpretation of the results. This choice, however, overlooks the classification of 'suberized' zones into 'patchy' and 'continuous' suberization (Barberon et al., 2016). Considering that the histological analysis of suberization in seedlings at 7 days after germination reported the most significant delay in suberization in the extent of the 'patchy' and 'continuous' regions (Cavaco, 2022) our results suggest that the start of the suberization of the endodermal cells does not seem affected by the absence of a functional *ANT* and that the *ant-9* delay in entrance in the continuous suberization of the endodermis and periderm happens later in development. Through the relative expression analysis of genes involved in the suberin biosynthesis and transport in *ant-9* compared to L*er*, our results showed that *ANT* is involved in the regulation of genes encoding key enzymes of the suberization pathway. The low levels, close to zero, of relative expression of suberization-related genes observed in stem tissue is consistent with the absence of suberization in the stem of Arabidopsis (Wunderling et al., 2018). The analysis of transcriptional levels on root-hypocotyl tissues provided evidence for an effect of the lack of *ANT* on the suberin biosynthesis, with a reduction in expression of *ASFT*, and the increased expression of *CYP86B1* indicating the effect of *ANT*, which seems to promote *ASFT* expression while controlling the production of long chain ω-hydroxy-fatty acids. The reduced transcriptional levels of *ASFT* are consistent with the hypothesis that *ANT* might be affecting the ABA pathway, however *CYP86B1* increase suggests the involvement of additional mechanisms (Choi & Kim, 2023).

4.3 *ANT* regulates suberization modulating the ABA pathway

Our preliminary experiment on the exogenous ABA supply on *ant-9* seedlings, despite the low sample numbers (6 *ant-9* individuals, 4 L*er* individuals), showed that ABA induces suberization in the *ant-9*, to a similar extent as in the wild-type. This experiment is inconclusive as to what extent ABA is capable of restoring the *ant-9* suberization delay since no significant differences were observed between L*er* and *ant-9* suberization in the 4-day seedlings. Possibly the significant differences reside in the proportion of continuous suberization and patchy suberization as it occurs at 7 days (Cavaco, 2022). Nevertheless, it is evident that ANT acts upstream of ABA. Interestingly, ANT is involved in the ABA signaling cascade under stress conditions, where ARF2 negatively regulates *ANT*, and in the presence of ABA the expression of *ANT* is induced (Meng et al., 2015). However, our transcriptional analysis of genes associated with the ABA pathway, showed that the lack of a functional *ANT* affects the ABA biosynthesis (reduced relative expression of *NCED3*) as well as ABA signaling (reduced expression of *PP2CA*).

The fact that suberization is delayed in *ant-9*, and the evidence suggesting the involvement of ANT in a feedback loop increasing ABA signaling, implies *ANT* is in fact, at least partially, regulating suberization by controlling the ABA biosynthesis and signaling. Yet, the effect of *ant-9* on the ABA pathway is unable to fully explain the effect on the suberin pathway gene expression observed, suggesting other mechanisms might be involved. A potential candidate is WRKY9 which induces *CYP86B1*, being regulated negatively by *ANT* (Choi & Kim, 2023; Krishnamurthy et al., 2021). However, this relationship remains to be investigated in future experiments.

5 Conclusions & Future Perspectives

The WOX9 and ANT transcription factors identified in cork oak and studied in Arabidopsis suggested their involvement in the suberization process during early root development. Our findings indicate that *WOX9*, known for regulating meristematic cell proliferation, acts as a positive regulator of the ABA biosynthesis and strongly affects the ABA signaling in late stages of development, corroborating previous results from our lab. Given the versatility of ABA in controlling both developmental and environmental-induced suberization perhaps *WOX9* is part of a more complex module, regulating the ABA-dependent control of suberization through affecting its perception or signaling, Other WUSCHEL transcription factors are known to operate in such signaling regulatory modules. *WOX4*, for instance, operates in a central signaling module that regulates the auxin-dependent lateral growth (of the vascular cambium) involving CLE41 peptide and PXY RLK (Etchells et al., 2013). It is tempting to speculate *WOX9* could be part of such a complex signaling module in the control of the ABA-dependent cork cambium development. Further studies will be needed. We also successfully built a genetic construct to allow the study of functional similarities between AtWOX9 and QsWOX9, further research is required to determine whether the AtWOX9 and QsWOX9 homologs have similar functions.

ANT, which is involved fin floral organ and vascular cambium development, seems to also be involved in phellogen development in Arabidopsis. Here we showed that although the *ant-9* delay in endodermis suberization is unnoticeable in early developmental stages, in later stages of root development, ANT affects the expression of suberization-associated genes in roots, and suberization in *ant-9* mutants can be induced by ABA exogenous supply. The expression analysis of genes encoding enzymes relevant in the ABA pathway revealed *ANT* as a positive regulator of the ABA biosynthesis and signaling. *ANT* is known to target several genes involved in auxin-signaling (Krizek et al., 2020). It would be interesting to search for targets of *ANT* that might be involved in regulating ABA signaling. It is possible that *ANT* is affecting the suberization through other mechanisms as well, therefore the future investigation of interactions with other candidates, such as WRKY-family members, might help elucidate the regulatory mechanisms involving *ANT*.

These results provide an advancement towards the characterization of the regulatory mechanisms, involving *WOX9* and *ANT*, underlying the suberin barrier formation in the endodermal and periderm cells during phellogen development.

6 References

Altschul, S. F., Madden, T. L., Schäffer, A. A., Zhang, J., Zhang, Z., Miller, W., & Lipman, D. J. (1997). Gapped BLAST and PSI-BLAST: a new generation of protein database search programs. In *Nucleic Acids Research* (Vol. 25, Issue 17). Oxford University Press.

Andersen, T. G., Barberon, M., & Geldner, N. (2015). Suberization-the second life of an endodermal cell. In *Current Opinion in Plant Biology* (Vol. 28, pp. 9–15). Elsevier Ltd. https://doi.org/10.1016/j.pbi.2015.08.004

Andersen, T. G., Molina, D., Kilian, J., Franke, R. B., Ragni, L., & Geldner, N. (2021). Tissue-Autonomous Phenylpropanoid Production Is Essential for Establishment of Root Barriers. *Current Biology*, *31*(5), 965-977.e5. https://doi.org/10.1016/j.cub.2020.11.070

Barberon, M. (2017). The endodermis as a checkpoint for nutrients. In *New Phytologist* (Vol. 213, Issue 4, pp. 1604–1610). Blackwell Publishing Ltd. https://doi.org/10.1111/nph.14140

Barberon, M., Vermeer, J. E. M., De Bellis, D., Wang, P., Naseer, S., Andersen, T. G., Humbel, B. M., Nawrath, C., Takano, J., Salt, D. E., & Geldner, N. (2016). Adaptation of Root Function by Nutrient-Induced Plasticity of Endodermal Differentiation. *Cell*, *164*(3), 447–459. https://doi.org/10.1016/j.cell.2015.12.021

Belsson, F., Li, Y., Bonaventura, G., Pollard, M., & Ohlrogge, J. B. (2007). The acyltransferase GPAT5 is required for the synthesis of suberin in seed coat and root of Arabidopsis. *Plant Cell*, *19*(1), 351–368. https://doi.org/10.1105/tpc.106.048033

Brundrett, M. C., Kendrick, B., & Peterson, C. A. (1991). Efficient lipid staining in plant material with Sudan red 7b or fluoral yellow 088 in polyethylene glycol-glycerol. *Biotechnic and Histochemistry*, *66*(3), 111–116. https://doi.org/10.3109/10520299109110562

Campilho, A., Nieminen, K., & Ragni, L. (2020). The development of the periderm: the final frontier between a plant and its environment. In *Current Opinion in Plant Biology* (Vol. 53, pp. 10–14). Elsevier Ltd. https://doi.org/10.1016/j.pbi.2019.08.008

Cavaco, M. (2022). *Patterns of suberization in root tissues of Arabidopsis thaliana mutants* [Master's thesis, University of Lisbon]. Repositório da Universidade de Lisboa. http://hdl.handle.net/10451/56537

Chang, S., Puryear, J., & Cairney, J. (1993). A Simple and Efficient Method for Isolating RNA from Pine Trees. *Plant Molecular Biology Reporter*, *11*(2), 113–116.

Chan, Z. (2012). Expression profiling of ABA pathway transcripts indicates crosstalk between abiotic and biotic stress responses in Arabidopsis. *Genomics*, *100*(2), 110–115. https://doi.org/10.1016/j.ygeno.2012.06.004

Choi, J., & Kim, H. (2023). Disruption of the ABA1 encoding zeaxanthin epoxidase caused defective suberin layers in Arabidopsis seed coats. *Frontiers in Plant Science*, *14*. https://doi.org/10.3389/fpls.2023.1156356

Clough, S. J., & Bent, A. F. (1998). Floral dip: A simplified method for Agrobacterium-mediated transformation of *Arabidopsis thaliana*. *Plant Journal*, *16*(6), 735–743. https://doi.org/10.1046/j.1365-313X.1998.00343.x

Cohen, H., Fedyuk, V., Wang, C., Wu, S., & Aharoni, A. (2020). SUBERMAN regulates developmental suberization of the Arabidopsis root endodermis. In *Plant Journal* (Vol. 102, Issue 3, pp. 429–430). Blackwell Publishing Ltd. https://doi.org/10.1111/tpj.14785

Compagnon, V., Diehl, P., Benveniste, I., Meyer, D., Schaller, H., Schreiber, L., Franke, R., & Pinot, F. (2009). CYP86B1 is required for very long chain ω-hydroxyacid and α,ω-dicarboxylic acid synthesis in root and seed suberin polyester. *Plant Physiology*, *150*(4), 1831–1843. https://doi.org/10.1104/pp.109.141408

De Bellis, D., Kalmbach, L., Marhavy, P., Daraspe, J., Geldner, N., & Barberon, M. (2022). Extracellular vesiculo-tubular structures associated with suberin deposition in plant cell walls. *Nature Communications*, *13*(1). https://doi.org/10.1038/s41467-022-29110-0

Domergue, F., Vishwanath, S. J., Joubès, J., Ono, J., Lee, J. A., Bourdon, M., Alhattab, R., Lowe, C., Pascal, S., Lessire, R., & Rowland, O. (2010). Three Arabidopsis fatty Acyl-coenzyme a reductases, FAR1, FAR4, and FAR5, generate primary fatty alcohols associated with suberin deposition. *Plant Physiology*, *153*(4), 1539–1554. https://doi.org/10.1104/pp.110.158238

Efetova, M., Zeier, J., Riederer, M., Lee, C. W., Stingl, N., Mueller, M., Hartung, W., Hedrich, R., & Deeken, R. (2007). A central role of abscisic acid in drought stress protection of Agrobacterium-induced tumors on Arabidopsis. *Plant Physiology*, *145*(3), 853–862. https://doi.org/10.1104/pp.107.104851

Elliott, R. C., Betzner, A. S., Huttner, E., Oakes, M. P., Tucker, W. Q. J., Gerentes, D., Perez, P., & Smytha, D. R. (1996). AINTEGUMENTA, an A PETA LAP-like Gene of Arabidopsis with Pleiotropic Roles in Ovule Development and Floral Organ Growth. In *The Plant Cell* (Vol. 8). American Society of Plant Physiologists.

Etchells, J. P., Provost, C. M., Mishr, L., & Turner, S. R. (2013). WOX4 and WOX14 act downstream of the PXY receptor kinase to regulate plant vascular proliferation independently of any role in vascular organisation. *Development (Cambridge)*, *140*(10), 2224–2234. https://doi.org/10.1242/dev.091314

Evert, R. Franklin., Esau, K., & Esau, K. (2006). *Esau's Plant anatomy : meristems, cells, and tissues of the plant body : their structure, function, and development*. Wiley-Interscience.

Fich, E. A., Segerson, N. A., & Rose, J. K. C. (2016). The Plant Polyester Cutin: Biosynthesis, Structure, and Biological Roles. In *Annual Review of Plant Biology* (Vol. 67, pp. 207–233). Annual Reviews Inc. https://doi.org/10.1146/annurev-arplant-043015-111929

Geldner, N. (2013). The endodermis. In *Annual Review of Plant Biology* (Vol. 64, pp. 531–558). https://doi.org/10.1146/annurev-arplant-050312-120050

Gou, M., Hou, G., Yang, H., Zhang, X., Cai, Y., Kai, G., & Liu, C. J. (2017). The MYB107 transcription factor positively regulates suberin biosynthesis. *Plant Physiology*, *173*(2), 1045–1058. https://doi.org/10.1104/pp.16.01614

Graça, J. (2015). Suberin: The biopolyester at the frontier of plants. In *Frontiers in Chemistry* (Vol. 3, Issue OCT). Frontiers Media S. A. https://doi.org/10.3389/fchem.2015.00062

Holloway, P. J. (1983). *SOME VARIATIONS IN THE COMPOSITION OF SUBERIN FROM THE CORK LAYERS OF HIGHER PLANTS* (Vol. 22, Issue 2).

Iuchi, S., Kobayashi, M., Taji, T., Naramoto, M., Seki, M., Kato, T., Tabata, S., Kakubari, Y., Yamaguchi-Shinozaki, K., & Shinozaki, K. (2001). Regulation of drought tolerance by gene manipulation of 9-cis-epoxycarotenoid dioxygenase, a key enzyme in abscisic acid biosynthesis in Arabidopsis. *Plant Journal*, *27*(4), 325–333. https://doi.org/10.1046/j.1365-313X.2001.01096.x

Kamiya, T., Borghi, M., Wang, P., Danku, J. M. C., Kalmbach, L., Hosmani, P. S., Naseer, S., Fujiwara, T., Geldner, N., & Salt, D. E. (2015). The MYB36 transcription factor orchestrates Casparian strip formation. *Proceedings of the National Academy of Sciences of the United States of America*, *112*(33), 10533–10538. https://doi.org/10.1073/pnas.1507691112

Kim, S., Soltis, P. S., Wall, K., & Soltis, D. E. (2006). Phylogeny and domain evolution in the APETALA2-like gene family. *Molecular Biology and Evolution*, *23*(1), 107–120. https://doi.org/10.1093/molbev/msj014

Kolattukudy, P. E., Kronman, K., & Poulose, A. J. (1975). Determination of Structure and Composition of Suberin from the Roots of Carrot, Parsnip, Rutabaga, Turnip, Red Beet, and Sweet Potato by Combined Gas-Liquid Chroma-tography and Mass Spectrometry'. In *Plant Physiol* (Vol. 55). https://academic.oup.com/plphys/article/55/3/567/6074531

Kosma, D. K., Molina, I., Ohlrogge, J. B., & Pollard, M. (2012). Identification of an Arabidopsis fatty alcohol: Caffeoyl-Coenzyme a acyltransferase required for the synthesis of alkyl hydroxycinnamates in root waxes. *Plant Physiology*, *160*(1), 237–248. https://doi.org/10.1104/pp.112.201822

Kosma, D. K., Murmu, J., Razeq, F. M., Santos, P., Bourgault, R., Molina, I., & Rowland, O. (2014). AtMYB41 activates ectopic suberin synthesis and assembly in multiple plant species and cell types. *Plant Journal*, *80*(2), 216–229. https://doi.org/10.1111/tpj.12624

Krishnamurthy, P., Vishal, B., Bhal, A., & Kumar, P. P. (2021). WRKY9 transcription factor regulates cytochrome P450 genes CYP94B3 and CYP86B1, leading to increased root suberin and salt tolerance in Arabidopsis. *Physiologia Plantarum*, *172*(3), 1673–1687. https://doi.org/10.1111/ppl.13371

Krishnamurthy, P., Vishal, B., Ho, W. J., Lok, F. C. J., Lee, F. S. M., & Kumar, P. P. (2020). Regulation of a cytochrome P450 gene CYP94B1 by WRKY33 transcription factor controls apoplastic barrier formation in roots to confer salt tolerance. *Plant Physiology*, *184*(4), 2199–2215. https://doi.org/10.1104/pp.20.01054

Krizek, B. A. (2009). AINTEGUMENTA and AINTEGUMENTA-LIKE6 act redundantly to regulate Arabidopsis floral growth and patterning. *Plant Physiology*, *150*(4), 1916–1929. https://doi.org/10.1104/pp.109.141119

Krizek, B. A., Blakley, I. C., Ho, Y. Y., Freese, N., & Loraine, A. E. (2020). The Arabidopsis transcription factor AINTEGUMENTA orchestrates patterning genes and auxin signaling in the establishment of floral growth and form. *Plant Journal*, *103*(2), 752–768. https://doi.org/10.1111/tpj.14769

Krzywińska, E., Kulik, A., Bucholc, M., Fernandez, M. A., Rodriguez, P. L., & Dobrowolska, G. (2016). Protein phosphatase type 2C PP2CA together with ABI1 inhibits SnRK2.4 activity and regulates plant responses to salinity. *Plant Signaling and Behavior*, *11*(12). https://doi.org/10.1080/15592324.2016.1253647

Kuhn, J. M., Boisson-Dernier, A., Dizon, M. B., Maktabi, M. H., & Schroeder, J. I. (2006). The protein phosphatase AtPP2CA negatively regulates abscisic acid signal transduction in Arabidopsis, and effects of abh1 on AtPP2CA mRNA. *Plant Physiology*, *140*(1), 127–139. https://doi.org/10.1104/pp.105.070318

Kushiro, T., Okamoto, M., Nakabayashi, K., Yamagishi, K., Kitamura, S., Asami, T., Hirai, N., Koshiba, T., Kamiya, Y., & Nambara, E. (2004). The Arabidopsis cytochrome P450 CYP707A encodes ABA 8′-hydroxylases: Key enzymes in ABA catabolism. *EMBO Journal*, *23*(7), 1647–1656. https://doi.org/10.1038/sj.emboj.7600121

Lashbrooke, J., Cohen, H., Levy-Samocha, D., Tzfadia, O., Panizel, I., Zeisler, V., Massalha, H., Stern, A., Trainotti, L., Schreiber, L., Costa, F., & Aharoni, A. (2016). MYB107 and MYB9 homologs regulate suberin deposition in angiosperms. *Plant Cell*, *28*(9), 2097–2116. https://doi.org/10.1105/tpc.16.00490

Leal, A. R., Sapeta, H., Beeckman, T., Barros, P. M., & Oliveira, M. M. (2022). Spatiotemporal development of suberized barriers in cork oak taproots. *Tree Physiology*, *42*(6), 1269–1285. https://doi.org/10.1093/treephys/tpab176

Lopes, S. T., Sobral, D., Costa, B., Perdiguero, P., Chaves, I., Costa, A., & Miguel, C. M. (2020). Phellem versus xylem: Genome-wide transcriptomic analysis reveals novel regulators of cork formation in cork oak. *Tree Physiology*, *40*(2), 129–141. https://doi.org/10.1093/treephys/tpz118

Lux, A., Morita, S., Abe, J., & Ito, K. (2005). An improved method for clearing and staining free-hand sections and whole-mount samples. *Annals of Botany*, *96*(6), 989–996. https://doi.org/10.1093/aob/mci266

Machado, A., Pereira, H., & Teixeira, R. T. (2013). Anatomy and development of the endodermis and phellem of quercus suber l. roots. *Microscopy and Microanalysis*, *19*(3), 525–534. https://doi.org/10.1017/S1431927613000287

Mahmood, K., Zeisler-Diehl, V. V., Schreiber, L., Bi, Y. M., Rothstein, S. J., & Ranathunge, K. (2019). Overexpression of ANAC046 promotes suberin biosynthesis in roots of *Arabidopsis thaliana*. *International Journal of Molecular Sciences*, *20*(24). https://doi.org/10.3390/ijms20246117

Meng, L. S., Wang, Z. B., Yao, S. Q., & Liu, A. (2015). The ARF2-ANT-COR15A gene cascade regulates ABA-signalingmediated resistance of large seeds to drought in Arabidopsis. *Journal of Cell Science*, *128*(21), 3922–3932. https://doi.org/10.1242/jcs.171207

Mizukami, Y., & Fischer, R. (2000). Plant organ size control: AINTEGUMENTA regulates growth and cell numbers during organogenesis. In *PNAS* (Vol. 97, Issue 2). www.pnas.org

Moire, L., Schmutz, A., Buchala, A., Yan, B., Stark, R. E., & Ryser, U. (1983). *Glycerol Is a Suberin Monomer. New Experimental Evidence for an Old Hypothesis 1*. Kerstiens. www.plantphysiol.org

Molina, I., Li-Beisson, Y., Beisson, F., Ohlrogge, J. B., & Pollard, M. (2009). Identification of an Arabidopsis feruloyl-coenzyme a transferase required for suberin synthesis. *Plant Physiology*, *151*(3), 1317–1328. https://doi.org/10.1104/pp.109.144907

Naseer, S., Lee, Y., Lapierre, C., Franke, R., Nawrath, C., & Geldner, N. (2012). Casparian strip diffusion barrier in Arabidopsis is made of a lignin polymer without suberin. *Proceedings of the National Academy of Sciences of the United States of America*, *109*(25), 10101–10106. https://doi.org/10.1073/pnas.1205726109

Nomberg, G., Marinov, O., Arya, G. C., Manasherova, E., & Cohen, H. (2022). The Key Enzymes in the Suberin Biosynthetic Pathway in Plants: An Update. In *Plants* (Vol. 11, Issue 3). MDPI. https://doi.org/10.3390/plants11030392

Park, S. Y., Fung, P., Nishimura, N., Jensen, D. R., Fujii, H., Zhao, Y., Lumba, S., Santiago, J., Rodrigues, A., Chow, T. F. F., Alfred, S. E., Bonetta, D., Finkelstein, R., Provart, N. J., Desveaux, D., Rodriguez, P. L., McCourt, P., Zhu, J. K., Schroeder, J. I., … Cutler, S. R. (2009). Abscisic acid inhibits type 2C protein phosphatases via the PYR/PYL family of START proteins. *Science*, *324*(5930), 1068–1071. https://doi.org/10.1126/science.1173041

Pereira, H. (2007). *Cork: Biology, Production and Uses* (pp. 7–127). Elsevier.

Pfaffl, M. W. (2001). A new mathematical model for relative quantification in real-time RT-PCR. In *Nucleic Acids Research* (Vol. 29, Issue 9).

Rains, M. K., De Silva, N. D. G., & Molina, I. (2018). Reconstructing the suberin pathway in poplar by chemical and transcriptomic analysis of bark tissues. *Tree Physiology*, *38*(3), 340–361. https://doi.org/10.1093/treephys/tpx060

Randall, R. S., Miyashima, S., Blomster, T., Zhang, J., Elo, A., Karlberg, A., Immanen, J., Nieminen, K., Lee, J. Y., Kakimoto, T., Blajecka, K., Melnyk, C. W., Alcasabas, A., Forzani, C., Matsumoto-Kitano, M., Mähönen, A. P., Bhalerao, R., Dewitte, W., Helariutta, Y., & Murray, J. A. H. (2015). AINTEGUMENTA and the D-type cyclin CYCD3;1 regulate root secondary growth and respond to cytokinins. *Biology Open*, *4*(10), 1229–1236. https://doi.org/10.1242/bio.013128

Sato, H., Takasaki, H., Takahashi, F., Suzuki, T., Iuchi, S., Mitsuda, N., Ohme-Takagi, M., Ikeda, M., Seo, M., Yamaguchi-Shinozaki, K., & Shinozaki, K. (2018). *Arabidopsis thaliana* NGATHA1 transcription factor induces ABA biosynthesis by activating NCED3 gene during dehydration stress. *Proceedings of the National Academy of Sciences of the United States of America*, *115*(47), E11178–E11187. https://doi.org/10.1073/pnas.1811491115

Schmidt, H. W., & Schönherr, J. (1982). Fine structure of isolated and non-isolated potato tuber periderm. In *Planta* (Vol. 154).

Serra, O., & Geldner, N. (2022). The making of suberin. In *New Phytologist* (Vol. 235, Issue 3, pp. 848–866). John Wiley and Sons Inc. https://doi.org/10.1111/nph.18202

Serra, O., Mähönen, A. P., Hetherington, A. J., & Ragni, L. (2022). The Making of Plant Armor: The Periderm. *Annual Review of Plant Biology*, *73*, 405–432. https://doi.org/10.1146/annurev-arplant-102720

Serra, O., Soler, M., Hohn, C., Franke, R., Schreiber, L., Prat, S., Molinas, M., & Figueras, M. (2009). Silencing of StKCS6 in potato periderm leads to reduced chain lengths of suberin and wax compounds and increased peridermal transpiration. *Journal of Experimental Botany*, *60*(2), 697–707. https://doi.org/10.1093/jxb/ern314

Serra, O., Soler, M., Hohn, C., Sauveplane, V., Pinot, F., Franke, R., Schreiber, L., Prat, S., Molinas, M., & Figueras, M. (2009). CYP86A33-targeted gene silencing in potato tuber alters suberin composition, distorts suberin lamellae, and impairs the periderm's water barrier function. *Plant Physiology*, *149*(2), 1050–1060. https://doi.org/10.1104/pp.108.127183

Shanmugarajah, K., Linka, N., Gräfe, K., Smits, S. H. J., Weber, A. P. M., Zeier, J., & Schmitt, L. (2019). ABCG1 contributes to suberin formation in *Arabidopsis thaliana* roots. *Scientific Reports*, *9*(1). https://doi.org/10.1038/s41598-019-47916-9

Shukla, V., Han, J.-P., Cléard, F., Lefebvre-Legendre, L., Gully, K., Flis, P., Berhin, A., Andersen, T. G., Salt, D. E., Nawrath, C., & Barberon, M. (2021). Suberin plasticity to developmental and exogenous cues is regulated by a set of MYB transcription factors. *Plant Biology*, *118*(39), 1–11. https://doi.org/10.1073/pnas.2101730118/-/DCSupplemental

Silva, S. P., Sabino, M. A., Fernandas, E. M., Correlo, V. M., Boesel, L. F., & Reis, R. L. (2005). Cork: Properties, capabilities and applications. In *International Materials Reviews* (Vol. 50, Issue 6, pp. 345–365). Maney Publishing. https://doi.org/10.1179/174328005X41168

Skylar, A., Hong, F., Chory, J., Weigel, D., & Wu, X. (2010). STIMPY mediates cytokinin signaling during shoot meristem establishment in Arabidopsis seedlings. *Development*, *137*(4), 541–549. https://doi.org/10.1242/dev.041426

Soler, M., Serra, O., Molinas, M., Huguet, G., Fluch, S., & Figueras, M. (2007). A genomic approach to suberin biosynthesis and cork differentiation. *Plant Physiology*, *144*(1), 419–431. https://doi.org/10.1104/pp.106.094227

Tan, B. C., Joseph, L. M., Deng, W. T., Liu, L., Li, Q. B., Cline, K., & McCarty, D. R. (2003). Molecular characterization of the Arabidopsis 9-cis epoxycarotenoid dioxygenase gene family. *Plant Journal*, *35*(1), 44–56. https://doi.org/10.1046/j.1365-313X.2003.01786.x

Untergasser, A., Cutcutache, I., Koressaar, T., Ye, J., Faircloth, B. C., Remm, M., & Rozen, S. G. (2012). Primer3-new capabilities and interfaces. *Nucleic Acids Research*, *40*(15). https://doi.org/10.1093/nar/gks596

Ursache, R., De Jesus Vieira Teixeira, C., Dénervaud Tendon, V., Gully, K., De Bellis, D., Schmid-Siegert, E., Grube Andersen, T., Shekhar, V., Calderon, S., Pradervand, S., Nawrath, C., Geldner, N., & Vermeer, J. E. M. (2021). Discovery of GDSL-domain proteins have key roles in suberin polymerization and degradation. *Nature Plants*, *7*(3), 353–364. https://doi.org/10.1038/s41477-021-00862-9

Vishwanath, S. J., Delude, C., Domergue, F., & Rowland, O. (2015). Suberin: biosynthesis, regulation, and polymer assembly of a protective extracellular barrier. In *Plant Cell Reports* (Vol. 34, Issue 4, pp. 573–586). Springer Verlag. https://doi.org/10.1007/s00299-014-1727-z

Wang, C., Wang, H., Li, P., Li, H., Xu, C., Cohen, H., Aharoni, A., & Wu, S. (2020). Developmental programs interact with abscisic acid to coordinate root suberization in Arabidopsis. *Plant Journal*, *104*(1), 241–251. https://doi.org/10.1111/tpj.14920

Wan, J., Wang, R., Zhang, P., Sun, L., Ju, Q., Huang, H., Lü, S., Tran, L. S., & Xu, J. (2021). MYB70 modulates seed germination and root system development in Arabidopsis. *IScience*, *24*(11). https://doi.org/10.1016/j.isci.2021.103228

Wunderling, A., Ripper, D., Barra-Jimenez, A., Mahn, S., Sajak, K., Targem, M. Ben, & Ragni, L. (2018). A molecular framework to study periderm formation in Arabidopsis. *New Phytologist*, *219*(1), 216–229. https://doi.org/10.1111/nph.15128

Wu, X., Dabi, T., & Weigel, D. (2005). Requirement of Homeobox Gene STIMPY/WOX9 for Arabidopsis Meristem Growth and Maintenance. *Current Biology*, *15*, 436–440. https://doi.org/10.1016/j

Yadav, V., Molina, I., Ranathunge, K., Castillo, I. Q., Rothstein, S. J., & Reed, J. W. (2014). ABCG transporters are required for suberin and pollen wall extracellular barriers in Arabidopsis. *Plant Cell*, *26*(9), 3569–3588. https://doi.org/10.1105/tpc.114.129049

Yoshida, T., Nishimura, N., Kitahata, N., Kuromori, T., Ito, T., Asami, T., Shinozaki, K., & Hirayama, T. (2006). ABA-hypersensitive germination3 encodes a protein phosphatase 2C (AtPP2CA) that strongly regulates abscisic acid signaling during germination among Arabidopsis protein phosphatase 2Cs. *Plant Physiology*, *140*(1), 115–126. https://doi.org/10.1104/pp.105.070128